

# **Volumetric atlasing in the rodent brain: connecting experimental image data to standard anatomical space**

by

**Eszter Agnes Papp**

A dissertation submitted to  
the University of Oslo  
for the degree of

**Philosophiae Doctor (Ph.D.)**

2017



Principal supervisor: Jan G. Bjaalie  
Co-supervisor: Trygve B. Leergaard

Division of Anatomy  
Department of Molecular Medicine  
Institute of Basic Medical Sciences  
University of Oslo

© **Eszter Agnes Papp, 2018**

*Series of dissertations submitted to the  
Faculty of Medicine, University of Oslo*

ISBN 978-82-8377-194-7

All rights reserved. No part of this publication may be  
reproduced or transmitted, in any form or by any means, without permission.

Cover: Hanne Baadsgaard Utigard.  
Print production: Reprosentralen, University of Oslo.

**ATLAS·ING** In the context of the present work, we refer to atlasing as the development and application of brain atlases and related software with the aim to facilitate integration and spatial analysis of various types of experimental data and maps from the brain based on anatomical location.



# TABLE OF CONTENTS

Acknowledgments .....	III
Publications .....	V
Abstract .....	VI
List of abbreviations .....	VII

## **Synopsis**

Introduction .....	1
Rodent brain reference atlases: 2D to 3D .....	2
Coordinate systems for brain atlasng .....	5
Assignment of anatomical location to experimental images .....	8
Towards data integration in the rodent brain .....	10
Aims .....	13
Material and methods .....	15
Ethical considerations .....	15
2D and 3D image material .....	17
Volumetric segmentation tools and procedures .....	19
Anatomical delineations .....	21
Waxholm Space coordinate system for the rat brain .....	23
Anatomical landmarks for image registration .....	26
Detection and spatial alignment of neuronal labeling .....	27
Data sharing and documentation .....	29
Results .....	31
Paper I .....	33
Paper II .....	35
Paper III .....	37

Discussion .....	39
Anatomical reference material .....	40
Delineations of white and gray matter .....	43
Spatial reference: Waxholm Space for the rat brain .....	46
Connecting experimental image data to standard atlas space .....	50
Standard landmark set in Waxholm Space .....	50
Alignment of microscopic image series to MRI .....	54
Localization of labeling in brain-wide microscopy datasets .....	56
Impact and adoption by the community .....	58
Conclusions .....	61
References .....	63
Appendix .....	75
Papers .....	87

## ACKNOWLEDGMENTS

The present study was carried out between 2010 and 2017 in the Neural Systems and Graphics Computing Laboratory, Division of Anatomy, Institute of Basic Medical Sciences, University of Oslo, Norway. The Institute provided me with training, computing resources, and office space, as well as a venue and community for scientific discussions.

I would like to express my sincere gratitude to my supervisors, Jan G. Bjaalie and Trygve B. Leergaard, without whom this PhD project would not have been possible. I appreciate that Jan was able to set apart time for discussions despite his fully booked calendar. I would also like to thank him for maintaining an optimistic mindset throughout the ups and downs of the project. He provided the vision for the research plan and connected our work to international research initiatives. I am grateful for many interesting and thought-provoking discussions with Trygve. He provided me with insight on the biological problems behind our research on numerous occasions, and he gave me very constructive and structured feedback about my writing. I also learned a lot from his presentations and from his advice on creating figures and posters.

Special thanks to Professor Arild Njå, who followed my work from the initial research plan to the midterm review. I greatly appreciate his detailed and thoughtful comments on the manuscript. I would also like to thank the help of our collaborators, in particular Evan Calabrese and G. Allan Johnson for equipping us with the highest quality rat brain MRI and DTI available for the atlasing project, and Evan for his explanations about DTI contrasts. I had the opportunity to work together with members of the Digital Atlasing Task Force at the International Neuroinformatics Coordinating Facility. I am grateful for their insights and support. I would specifically like to thank Jyl Boline and Rembrandt Bakker for fruitful discussions, and James Gee and Paul Yushkevich for the ITK-SNAP software. Finally, I want to thank Marina Sergejeva for her work on landmark definition and testing, as well as her positive and helpful attitude throughout our collaboration.

I would like to acknowledge all members of the NeSys group for the welcoming atmosphere from the beginning of my stay in Norway. I especially appreciate the selfless practical help from Hong Qu and Kirsten Haga during my arrival. I would like to thank Trine Hjørnevik for her advice on 3D atlas reconstructions. Her thesis and defense have been an inspiration. Special thanks to fellow PhD students Lisa J. Kjørnigsen, Izabela M. Zakiewicz, and Sveinung Lillehaug.

I am grateful for the numerous travel opportunities throughout my PhD training to attend conferences, meetings, and courses within and outside Norway. I had the good fortune to receive a travel award from the US National Institutes of Health (grant R13 NS074833) to attend the Neuroinformatics 2011 conference in Boston, my first trip to the USA. I studied nanomedicine under the northern lights in Tromsø, and joined CMBN conferences in Hafjell and Geilo. I appreciate having been invited to several NeSys PhD retreats at Voksenkollen. I would like to thank the Norwegian Research School in Medical Imaging, and in particular Erik Ingebrigtsen, for the opportunity to attend MedIm conferences in Oslo, Trondheim, and Tromsø. I also enjoyed the seminars organized by the Nansen Neuroscience Network and the PhD forum at the Institute.

As additional sources of helpful tips and inspiration, I would like to mention the thesis guidelines shared by Steve Easterbrook from the University of Toronto, the thesis writing blog of Dora Farkas, and the PhD comics and movies created by Jorge Cham.

Finally, I wish to thank my partner, Gergely Csúcs, for following me to Norway and for his patience and support throughout the long years of completing my thesis. His work on atlas visualization and alignment software, and our discussions about coordinate transformations have proven invaluable for publishing the Waxholm Space atlas of the Sprague Dawley rat brain.

Oslo, August 2017

Eszter A. Papp



## PUBLICATIONS

- I. Papp EA, Leergaard TB, Calabrese E, Johnson GA, Bjaalie JG  
**Waxholm Space atlas of the Sprague Dawley rat brain**  
NeuroImage 97 (2014) 374-386.  
DOI: [10.1016/j.neuroimage.2014.04.001](https://doi.org/10.1016/j.neuroimage.2014.04.001)  
  
Papp EA, Leergaard TB, Calabrese E, Johnson GA, Bjaalie JG  
**Addendum to “Waxholm Space atlas of the Sprague Dawley rat brain” [NeuroImage 97 (2014) 374-386]**  
NeuroImage 105 (2015) 561–562.  
DOI: [10.1016/j.neuroimage.2014.10.017](https://doi.org/10.1016/j.neuroimage.2014.10.017)
- II. Sergejeva M, Papp EA, Bakker R, Gaudnek MA, Okamura-Oho Y, Boline J, Bjaalie JG, Hess A  
**Anatomical landmarks for registration of experimental image data to volumetric rodent brain atlasing templates**  
Journal of Neuroscience Methods 240 (2015) 161-169.  
DOI: [10.1016/j.jneumeth.2014.11.005](https://doi.org/10.1016/j.jneumeth.2014.11.005)
- III. Papp EA, Leergaard TB, Csucs G, Bjaalie JG  
**Brain-wide mapping of axonal connections: workflow for automated detection and spatial analysis of labeling in microscopic sections**  
Frontiers in Neuroinformatics (2016) 10:11  
DOI: [10.3389/fninf.2016.00011](https://doi.org/10.3389/fninf.2016.00011)

## ABSTRACT

A major challenge for understanding the brain in health and disease is related to combining information about the brain from many different sources. Spatial analysis and comparison of 2D and 3D brain images with the aim to discover new structural and functional features in the data requires mapping the images to a common anatomical space. For rodent models, widely used anatomical reference atlases have until recently been published in a book format that hinders effective comparison across images acquired at different angles and dimensions. The ambition of this study is to advance digital atlasing of the rodent brain towards a new generation of volumetric atlases that facilitate integration of whole-brain image data from multiple modalities.

We present the first comprehensive anatomical reference atlas of the Sprague Dawley rat brain based on magnetic resonance imaging. To ensure interoperability with other atlases, we applied the Waxholm Space standard in the rat brain for the first time, and created a mapping against the widely used stereotaxic space. For connecting experimental data to the new reference atlas, we established standard anatomical landmarks for image registration across different levels of structural detail, and created a workflow for section to volume alignment and spatial analysis of brain-wide microscopic image series. Open access to the results of this work has enabled localization of signal in functional and structural image volumes, integration of 2D image series, and development of new atlases of various features of the brain.

## LIST OF ABBREVIATIONS

2D, 3D	Two-dimensional, three-dimensional
BDA	Biotinylated dextran amine
BIRN	Biomedical Informatics Research Network
CC-BY-NC-SA	Creative Commons Attribution-NonCommercial-ShareAlike
CT	Computed tomography
dMRI	Diffusion-weighted magnetic resonance imaging
DOI	Digital Object Identifier
DTI	Diffusion tensor imaging
DWI	Diffusion-weighted image
FA	Fractional anisotropy
fMRI	Functional magnetic resonance imaging
INCF	International Neuroinformatics Coordinating Facility
ITK-SNAP	Insight Segmentation and Registration Toolkit Snake Automatic Partitioning
$\mu$ CT	Microscopic resolution computed tomography
MBAT	Mouse BIRN Atlasing Toolkit
MRI	Magnetic resonance imaging
NifTI	Neuroimaging Informatics Technology Initiative
NITRC	Neuroimaging Informatics Tools and Resources Clearinghouse
PET	Positron emission tomography
<i>Pha-L</i>	<i>Phaseolus vulgaris</i> leucoagglutinin
WHS	Waxholm Space
XML	Extended markup language



# **SYNOPSIS**



# INTRODUCTION

The brain is the most complex living structure known. From the level of gene expression and intracellular processes to the level of synapses, neurons, neural circuits, and the connectome, the brain presents several layers of organization. Uncovering the constructional and operational principles of each layer is central to understanding the brain in health and disease, and identifying strategies for prevention, diagnosis, and treatment of disorders, injuries and developmental defects of the brain. A variety of imaging methods and experimental techniques are used in neuroscience for exploring this complex biological system, covering spatial scales from molecular and cellular levels to the level of brain regions and the whole brain (Grignon et al. 2012; Hillman, 2007; Hurley and Taber, 2008; Otte and Halsband, 2006; Venneti et al. 2013). Since each of these techniques captures only specific aspects of brain structure or function, it is necessary to combine results from different types of measurements to get a more complete picture. Compiling such heterogeneous data into searchable, comparable and interpretable information, referred to as data integration, represents a major challenge for neuroscience as recognized by ongoing international research programs, including the Human Brain Project ([www.humanbrainproject.eu](http://www.humanbrainproject.eu)) and the BRAIN Initiative ([www.braininitiative.nih.gov](http://www.braininitiative.nih.gov)).

A common trait across datasets acquired from the brain is spatial relatedness. Anatomical location therefore provides a natural basis for organizing diverse types of measurement results (Van Essen, 2002). Assembly of data into a common space requires a standard anatomical, spatial and semantic reference to be defined, and methodology and tools for alignment of images to this reference. Brain atlases form the central pillar of such an integration space (Toga, 2002). In addition to maps of anatomical boundaries, reference atlases offer standard coordinate systems for navigation and measurements, and connect new findings to existing information about the brain through established nomenclatures.

Having their foundation laid upon anatomical images, reference atlases are also a plausible starting point for image alignment procedures. With a focus on rodents as experimental models, the following chapters briefly review the current state of brain atlasing from a data integration standpoint. We explore available resources with regard to reference material and atlas formats, coordinate systems, and image alignment in order to identify key development directions towards brain-wide spatial integration of experimental data.

### **Rodent brain reference atlases: 2D to 3D**

The most widely used atlases of the rodent brain are stereotaxic atlases designed to aid localization of features observed in microscopic images and planning of surgical procedures such as the placement of electrodes into the brain (Dong, 2008; Franklin and Paxinos, 2008; Paxinos and Watson, 2007; Swanson, 2004). These atlases consist of series of plates delineating anatomical details observed in histological material stained for cyto-, chemo-, or myeloarchitecture. The atlas plates provide cross-sectional views of the brain along standard coronal, sagittal and horizontal planes, arranged in a book format. Since the analysis of obliquely cut microscopic sections is not supported by this format, surface reconstructions have been created from anatomical delineations presented in stereotaxic atlases of both rat and mouse (Hjornevik et al. 2007; Leergaard et al. 2003; Majka et al. 2012, 2013), and slicing software were developed to generate atlas plates cut at arbitrary angles (Elsevier BrainNavigator, <http://www.abe.pl/en/resources/databases/brainnav>; Allen Institute Brain Explorer, <http://mouse.brain-map.org/static/brainexplorer>). For compatibility with tomographic images of the brain, volumetric atlas reconstructions are used (Hjornevik et al. 2007; Nie et al. 2013; Schwarz et al. 2006; Valdes-Hernandez et al. 2011), or the experimental image volumes are transformed to replicate the size and viewing angle of the stereotaxic atlas plates (Johnson et al. 2012; Lu et al. 2010; Schweinhardt et al. 2003).



Due to recent developments in 3D imaging, the format of reference atlases has evolved from series of 2D plates towards 3D volumes of the brain. An increase in the resolution of magnetic resonance imaging (MRI) and diffusion tensor imaging (DTI) to the scale of tens of microns has made it possible to perform volumetric anatomical mapping of the rodent brain based directly on image contrast (Badea et al. 2007; Chuang et al. 2011; Ma et al. 2005; Ma et al. 2008; Rumpel et al. 2013; Veraart et al. 2011). Magnetic susceptibility and water diffusion direction measurements yield structural images that reflect topological characteristics of brain tissue such as the size and distribution of cells, and the orientation and density of fibers (Alexander et al. 2007; Badea and Johnson, 2012). Anatomical information in these high resolution images can be used for building a volumetric atlas by assigning an anatomical label to each voxel that represents the brain. The resulting delineations share the same volumetric format as the underlying image template, providing direct spatial correspondence between the anatomical map and the MRI/DTI data.

The main advantage of using MRI to build reference atlases of the brain is the availability of morphologically correct anatomical images that display the same depth in all dimensions. Such material enables spatial alignment of both 2D and 3D datasets. *In situ* imaging leaves the cranial vault undisturbed and preserves the shape of the brain close to the *in vivo* situation, providing an ideal starting point for integration of images from modalities affected by tissue distortions, e.g. microscopy. Isotropic acquisition allows templates and associated delineations to be sliced dynamically at arbitrary angles. This feature is central to the alignment of microscopic image series to volumetric atlases. In addition to compatibility with 2D data, volume to volume alignment between the anatomical template and 3D images from other modalities makes it possible to use the volumetric delineations for localization of signal from *in vivo* functional and pharmacological images that show limited or no structural contrast.

Reference atlases, whether 2D or 3D, facilitate data integration by assembling anatomical information into a common space. Classical neuroanatomical atlases incorporate spatial information from multiple categories of histological material and key pieces of literature through a curation process that involves the selection and interpretation of disparate anatomical data. This type of integrative atlas is a result of an environment with limited access to image data and anatomical findings, and few computational resources to scale up data integration. The appearance of high-throughput data acquisition methods has led to the development of specialized open access atlases accumulating large amounts of data systematically collected for visualizing specific tissue elements or biomarkers throughout the brain. Examples of such atlas resources include the Allen Brain Atlas gene expression database for the mouse (Lein et al. 2007), the ViBrism transcriptome tomography database (Okamura-Oho et al. 2012), the Mouse Connectome Project (Hintiryan et al. 2012), the Allen Mouse Brain Connectivity Atlas (Oh et al. 2014), and the Whole Brain Connectivity Atlas for the rat (Zakiewicz et al. 2011). Data integration in this new distributed atlas environment can be defined as a means to connect diverse types of experimental data to both classical anatomical reference maps and specialized atlas resources in a way that any given anatomical location in one atlas translates to the same anatomical location in the other atlases. Being compatible with both 2D and 3D datasets from multiple modalities, MRI-based atlases have the potential to be used as spatial intermediaries between newly acquired data and existing atlases.

With this perspective in mind, volumetric atlases have recently been developed for two of the most widely used experimental rodent strains: the C57BL/6J mouse (Johnson et al. 2010) and the Wistar rat (Johnson et al. 2012). While based on microscopic resolution MRI, the level of detail in these atlases is limited to major brain regions and tracts, and delineation criteria are not provided. Without a detailed description of the anatomical basis of the delineations in the images, it is challenging to validate the anatomical boundaries and to extend these atlases, or evaluate their usability for a specific purpose. Building an MRI-based reference atlas for the Sprague Dawley strain, equally common in

laboratory use as the Wistar, with a consideration for these aspects will deepen our understanding of the extent high resolution MRI can be used for detailed brain-wide delineation of a larger number of structures, and thereby improve the utility of MRI-based atlases in general.

## **Coordinate systems for brain atlasing**

Anatomical delineations in a reference atlas subdivide the complete brain volume into smaller subvolumes by setting boundaries according to changes in cellular, biochemical or physical properties of the tissue. Nomenclature associated with these maps enables basic navigation across the brain at the level of areas, nuclei, regions, and tracts. For experimental and analytical procedures that necessitate a higher level of accuracy, or when a level of description independent of definitions of anatomical structures is required, local (Brevik et al. 2001) or global (Evans et al. 2012) coordinate systems are used. In most cases, reference atlases employ Cartesian-like coordinate systems that provide a three-dimensional perpendicular grid anchored to a few anatomical reference points. Depending on practical considerations for the use of the atlas, these anchor points may reside inside or outside the brain (Figure 1).

Reference atlases based on histological material, such as the Paxinos and Watson (1982) atlas of the rat brain and the Franklin and Paxinos (1997) atlas of the mouse brain have used the stereotaxic coordinate system consisting of a metric grid with three main reference points: bregma (the point of intersection of the sagittal cranial suture with the curve of best fit along the coronal suture), lambda (the midpoint of the curve of best fit along the lambdoid suture), and the midpoint of the interaural line (a non-cranial reference point). The 3D orientation of the grid is defined by the mid-sagittal plane, a horizontal plane containing both bregma and lambda (flat skull position), and a perpendicular coronal plane. Mediolateral coordinates are calculated from the midline, whereas anteroposterior and dorsoventral coordinates are measured from the reference points closest to the brain region of interest to minimize errors due to brain size variability in individual animals.

Reference atlases based on tomographic images have typically relied on internal landmarks in the brain for setting up a coordinate system, since cranial sutures are not readily recognized in most tomographic modalities with an exception for CT. The first widely used spatial standard built on internal reference points was developed for the human brain (Talairach et al. 1967). In this system, the anterior and the posterior commissure define the horizontal plane and the mid-sagittal plane is set to be vertical. Coordinates are calculated relative to the anterior commissure as the origin. The success of this approach lies in the observation that white to gray matter contrast is sufficient in most images for the commissures to be identified.

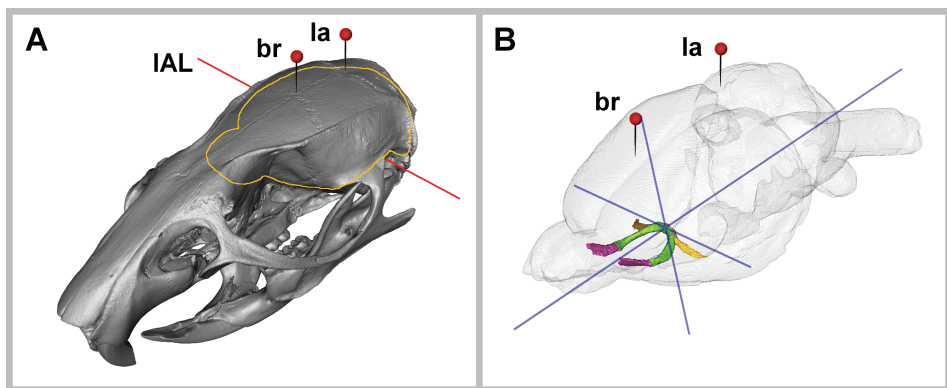


**Figure 1** | External and internal reference points in rodent brain atlasing.

**A:** Cranial landmarks bregma (**br**) and lambda (**la**), and the interaural line (**IAL**) are marked on a rat skull (volumetric rendering from  $\mu$ CT; DigiMorph Library, University of Texas at Austin). The position of the brain within the skull is indicated by a yellow line.

**B:** The axes of the Waxholm Space coordinate system (blue lines) are shown relative to the anterior commissure (structure in color). The position of bregma and lambda are marked above the brain surface (derived from the Waxholm Space atlas of the Sprague Dawley rat brain, Paper I).

As a result of the increasing use of high resolution small animal brain imaging, a similar atlasing standard based on internal reference points has become necessary for the rodent brain. The foundations of this new standard named Waxholm Space (WHS) have been laid down by the International Neuroinformatics Coordinating Facility (Hawrylycz et al. 2011). Waxholm Space is an image-based reference space comprised of two major components: a high quality anatomical template and an orthogonal coordinate system for navigating this volume. The primary entry point for experimental data into WHS is through image alignment to the anatomical target volume. Regions of interest are then assigned coordinates, allowing transformations to other coordinate systems and queries against WHS-mapped atlasing resources. The origin of the WHS coordinate system is set to the midpoint of the anterior commissure, making this spatial standard universally applicable across rodent species and strains, including most developmental stages. Waxholm Space is intended as a basis for a Digital Atlasing Infrastructure that connects atlasing resources and provides interoperability across spatial reference systems for advancing data integration in the rodent brain (Zaslavsky et al. 2014). As an initial step towards this vision, the WHS standard has been applied to a high resolution anatomical template of the C57BL/6J mouse brain (Johnson et al. 2010), enabling a mapping between multiple mouse atlases. A natural next step is to extend Waxholm Space to the rat brain. The rat is the preferred species for experimental studies in a number of areas in neuroscience, including the modeling of pharmacokinetics, neurological disorders, cognition and behavior. In addition, the implementation of Waxholm Space in the rat will offer interoperability towards gene expression data and developmental maps from mouse brain research, adding important analytical capabilities to rodent brain mapping.

## **Assignment of anatomical location to experimental images**

Interpretation of new observations from the brain captured in 2D or 3D experimental images requires the anatomical situation of the observed features to be identified. Alignment to a reference atlas establishes the spatial context for comparison across datasets and connects new findings to existing anatomical information. Numerous image processing techniques are available for transforming images into a common coordinate system (Zuk and Atkins, 1996). The choice of alignment method is influenced by i.a. the modality of the images, the level of contrast and anatomical detail, image dimensions (2D or 3D, slice or volume), and the availability of experimental metadata such as stereotaxic position or the angle of sectioning.

For classical section-based studies of the rodent brain, anatomical reference is typically obtained by manual alignment of individual section images to the best fitting plate in a stereotaxic atlas. To further aid the identification of specific anatomical regions, multiple images may be aligned to the same atlas plate, including images of neighboring sections or sections from comparable levels from other specimen stained to reveal landmark features or anatomical boundaries. The alignment procedure consists of several manual steps relying on visual observation of the images, utilizing 2D alignment functionality in common image editing software such as Adobe Photoshop, or specialized applications such as NeuroMaps (<http://braininfo.org>) and the Matlab-based Atlas Fitter (Kopec et al. 2011).

Due to the interactive nature of the alignment process, the above approach is best suited for a limited number of images. Alignment of large image datasets covering the whole brain, whether in the form of comprehensive series of microscopic images or volumetric data from tomographic modalities, requires automated registration methods that radically reduce the need for human interaction. Computer-assisted image alignment offers two main strategies for finding a match between images: intensity-based or feature-based registration.

Intensity-based alignment methods compare pixel- or voxel-level image information in order to transform the source image, e.g. a newly acquired experimental image, to the target (reference) image, i.e. an atlas. The wide-spread clinical use of volumetric imaging of the human brain over the last decades has resulted in an extensive library of algorithms for highly automated alignment of MRI, CT and PET images. These methods deliver optimal results when there is a high similarity between images, the target preferably being a high quality anatomical template. Limited anatomical contrast in the source image, or shape differences compared to the reference brain, in particular large-scale distortions typical in histology, represent challenges for intensity-based methods and require the use of a different approach.

Feature-based or landmark-based registration operates by matching a set of corresponding control points identified in both the source and the target image. Landmarks are characteristic image features such as edges, corners, or distinct shapes, in most cases simplified to a collection of points. Landmark-based alignment does not require the source and target images to be similar, provided that all landmarks can be distinguished in both images. Consequently, this approach can be applied in the integration of image data across modalities with variable level of structural detail and resolution. The prerequisite for successful alignment of different types of images to a common anatomical template is a standard set of landmarks reliably identifiable in all images, including the reference atlas. An example for the application of this strategy is the Talairach-Tournoux transformation used in human brain mapping (Talairach and Tournoux, 1988). In this system, eight landmark points are defined based on major white matter tracts (the anterior and the posterior commissure) and brain geometry (the outer extent of the brain along the mediolateral, anteroposterior and inferosuperior axes). The use of these landmarks allows fast global registration between whole-brain MRI scans. In rodent brain mapping a similar landmark system has not yet been introduced, but it would greatly aid integration of experimental images using the new generation of volumetric atlases.

## **Towards data integration in the rodent brain**

Different types of experimental results from the same brain region can be spatially related by registering data to an anatomical reference space. In this way, data are placed in a common context that allows researchers to answer queries about the distribution of anatomical, physiological, genetic, or other observations within and across regions, helping the planning and interpretation of experiments. However, it is technically difficult to combine data in a way that facilitates such discovery based research. The use of robotic equipment in histological processing and microscopic image acquisition, and recent resolution improvements in small animal volumetric imaging have led to a rapid expansion of whole-brain image material collected from rats and mice. While the benefits of an integrative analysis approach have been demonstrated previously using manual methods (Ungerstedt, 1971), the growing amount and diversity of data necessitates efficient analytical workflows employing automated procedures. Integration of datasets from multiple modalities requires a common anatomical reference space compatible with both 2D and 3D data. Reference atlases published in the classical book format are difficult to combine with automated image analysis procedures, and their utility is restricted by the use of standard cutting planes and the spacing between atlas plates. In addition, volumetric reconstructions of book atlases built for region of interest-based analysis of 3D datasets cannot be routinely shared due to copyright. For multimodal data integration to be successful, a new type of reference atlas is needed.

MRI-based atlases represent a new generation of 3D atlases that provide morphologically correct anatomical reference suitable for alignment of both 2D and 3D datasets across different levels of detail. In order for volumetric atlases to be used as a basis for data integration, they need to be equipped with comprehensive delineations covering the whole brain, and a spatial reference system anchored within the brain but interoperable with the stereotaxic system. Scaling up data integration on a community basis requires free access to data and atlasing resources. Therefore, atlases need to be not only 3D, but also publicly accessible and open for expansion and reinterpretation, with documentation



provided of the anatomical basis of the delineations. None of the currently available MRI-based rodent brain atlases fulfill all of these criteria.

Data integration in the 3D anatomical space of the new image-based reference atlases challenges current methods and workflows used for assignment of anatomical location to rodent brain data, in particular large series of microscopic images. While software are generally available for registration between volumetric datasets, spatial alignment across images differing in dimensions (2D to 3D) and modality (e.g. microscopy to MRI) is less widely explored. To view and analyze these datasets together, efficient section to volume alignment workflows with custom-angle slicing functionality are needed. Further, alignment of images with substantially different contrast or resolution is hindered by a lack of standard landmarks that can be recognized across image modalities. Complementing volumetric atlases with tools and methods that address these challenges will lower the threshold to the practical use of image-based reference atlases and associated spatial standards such as Waxholm Space, and demonstrate the potential of the new atlas format in spatial analysis of large microscopy datasets.



## AIMS

The overall aim of the present thesis is to contribute to the integration of experimental image data from the rodent brain, in particular whole-brain image volumes and series of microscopic images, by developing new atlasing resources and tools for connecting the images to standard anatomical space.

To address the challenges presented in the previous chapter, we have formulated the following specific goals:

1. Build a comprehensive open access atlas of the Sprague Dawley rat brain based on high resolution volumetric image material, and share the associated anatomical delineation criteria in detail.
2. Implement the Waxholm Space atlasing standard in the new rat brain atlas, and ensure interoperability between the resulting coordinate space and the stereotaxic system.
3. Identify a standard set of anatomical landmarks in the rodent brain for alignment of whole-brain experimental image data to mouse and rat Waxholm Space.
4. Demonstrate the use of the new reference atlas for spatial integration and region of interest-based analysis of microscopic image series with brain-wide coverage.



## MATERIAL AND METHODS

We used digital 2D and 3D images from the brains of rats and mice as the principal material in this study. Some of the images were reused from previously published datasets shared in online data repositories ([rbwb.org](http://rbwb.org), [software.incf.org](http://software.incf.org)). Technical details concerning experimental procedures, image acquisition, and image processing are described in the individual papers. The following section gives an overview of the experimental animals and procedures leading up to imaging, and the types of images acquired. We then explain how the images were used in producing the main results of this thesis, in particular anatomical delineations, implementation of the Waxholm Space coordinate system for the rat brain, identification of anatomical landmarks for image registration, and software for image processing and spatial alignment of large microscopic datasets.

### **Ethical considerations**

Research conducted in relation to the present work was performed along the guidelines for research ethics laid down in the 1974 Declaration of Helsinki. The responsibility of researchers to report methods and results accurately was addressed by publishing the enclosed research articles in peer-reviewed journals. The peer-review process contributes to quality control and ensuring the originality of research, and handles potential conflicts of interest.

Experimental material from several laboratory animals were used for the individual studies in this thesis (Table 1). The number of animals used for experiments was kept at a minimum. Close to half of the image material was reused from previously published datasets. Surgery was conducted on some of the animals to inject axonal tracers in specific brain regions, and perfusion was applied in some cases before imaging.

**Table 1** | Overview of experimental animals, procedures and imaging

Purpose of material	Nr.	Animal	Strain	Source	Experimental procedures	Imaging
Anatomical delineations (I.)	1	Rat	Sprague Dawley	Acq. CIVM	Perfusion (Gadoteridol)	MRI T <sub>2</sub> , T <sub>2</sub> <sup>*</sup> , DTI
Landmark identification (II.)	1	Mouse	C57BL/6J	WMA	Perfusion (Gadoteridol), Nissl	MRI T <sub>1</sub> , T <sub>2</sub> , T <sub>2</sub> <sup>*</sup> , microscopy
	2	Mouse	C57BL/6J	Acq. FAU	MnCl <sub>2</sub> i.p., CO <sub>2</sub> chamber	MRI T <sub>1</sub> , T <sub>2</sub> , T <sub>2</sub> <sup>*</sup>
	1	Mouse	C57BL/6J	Acq. RIKEN	Perfusion, cryosectioning	Block-face
Cranial landmark analysis (II.)	4	Mouse	C57BL/6J	Acq. FAU	CO <sub>2</sub> chamber	MRI T <sub>2</sub> , $\mu$ CT
Workflow for spatial analysis (III.)	2	Rat	Wistar	WBCA R601-R602	BDA tracing, perfusion, Nissl	Microscopy
	4	Rat	Sprague Dawley	WBCA R603-R606	BDA or Pha-L tracing, perfusion, Nissl	Microscopy

**Acq.** Newly acquired material

**CIVM** Duke Center for In Vivo Microscopy, USA

**FAU** Friedrich-Alexander University, Erlangen, Germany

**i.p.** Intraperitoneal injection

**RIKEN** RIKEN Advanced Science Institute, Japan

**WBCA** Whole Brain Connectivity Atlas, [rbwb.org](http://rbwb.org)

**WMA** Waxholm Mouse Atlas, [software.incf.org](http://software.incf.org)

Roman numerals in brackets point to Papers I-III.

All surgery was performed aseptically under deep anesthesia with the animal kept insensitive to pain throughout the procedure, and every attempt was made to minimize pain and discomfort. Postoperative monitoring and care was provided to prevent infection and promote recovery from surgery. None of the animals were subjected to successive survival surgical procedures.

All animal handling and experiments were approved by the Institutional Animal Welfare Committee of the University of Oslo and the Norwegian Animal Research Authority, the Duke University Institutional Animal Care and Use Committee, and the Institutional Animal Care and Use Committee of the Regierungspräsidium Mittelfranken, respectively. Experimental procedures and surgery were performed in compliance with European Community regulations on animal well-being (European Communities Council Directive 86/609/EEC) and the National Institute of Health guidelines for the care and use of laboratory animals.

## **2D and 3D image material**

An overview of experimental animals, procedures, and the types of images acquired from each animal is provided in Table 1. Experimental material from a total of 15 animals (7 rats and 8 mice) was used. The material was collected and processed with a focus on preparing the brain tissue for imaging. High quality 3D anatomical images were acquired for delineation of regions, tracts, and nuclei throughout the brain, and identification of anatomical landmarks in the brain and on the skull. A collection of 2D and 3D images were selected for evaluating landmark visibility across modalities and building a workflow for anatomical alignment of image data. Image acquisition methods and preparatory steps leading to imaging were chosen according to each of these specific aims.

High resolution contrast-enhanced *ex vivo* magnetic resonance images from 4 healthy adult male animals (1 rat and 3 mice) were used for atlasing and landmark identification. Three of the datasets were newly acquired, and one of the mouse templates was reused from a recently published atlasing study (Johnson et al. 2010). In preparation for imaging, the animals were deeply anesthetized, treated with an MRI contrast enhancing agent, and euthanized. Images with different types of MRI contrasts were collected in a continuous session for each animal, resulting in co-registered images. The goal of the imaging procedures was to produce high quality anatomical images with below hundred micrometer resolution in that the contrast and level of detail allows precise identification of anatomical regions, tracts, and landmark features throughout the brain. The isotropic volumes of the Waxholm mouse and rat templates were further used in the development of an interactive alignment tool that generates custom-angle atlas plates.

A variety of 2D and 3D images were collected from healthy adult rats and mice for testing anatomical landmarks for image registration. We used whole-brain image series and volumes from a range of image modalities that emphasize different characteristics of brain tissue. The image collection included block-face images of an unstained cryosectioned brain from transcriptome tomography, microscopic images of histological sections with and without cytoarchitectural counterstaining, contrast-enhanced anatomical MRI, and microscopic resolution computed tomography ( $\mu$ CT) aimed at cranial landmark analysis.

We re-used microscopic image series from brain-wide axonal tracing experiments shared through the Whole Brain Connectivity Atlas ([rbwb.org](http://rbwb.org); Zakiewicz et al. 2011) in the design and evaluation of a workflow for assigning anatomical location to neuronal labeling. Brightfield images of histological material from a total of 6 rats with cerebrocortical injections of biotinylated dextran amine (BDA) or *Phaseolus vulgaris* leucoagglutinin (*Pha-L*) were used. In addition to visualization of the axonal tracers, most sections were counterstained with thionine or Neutral Red to highlight cytoarchitecture.



## **Volumetric segmentation tools and procedures**

We used isotropic contrast-enhanced  $T_2$  and  $T_2^*$ -weighted MRI and fractional anisotropy-encoded primary eigenvector images (DTI) from a Sprague Dawley rat as the anatomical template for building a comprehensive structural atlas of the rat brain (Paper I). *Ex vivo* imaging of the whole head of the animal was performed with the brain residing intact in the skull. The images include most of the head except for the most anterior parts of the face and nose. In addition to the MRI and DTI, we used microscopic images of histological sections from comparable animals stained for myelin and cytoarchitecture to aid delineation decisions concerning white and gray matter.

The volumetric delineations were created using ITK-SNAP v2.2.0 (Insight Segmentation and Registration Toolkit Snake Automatic Partitioning, [www.itksnap.org](http://www.itksnap.org)), open source software funded by the U.S. National Institutes of Health for segmentation of medical images with several neuroscience applications (see e.g. Brun et al. 2009; Knickmeyer et al. 2008; Rumble et al. 2013; Veraart et al. 2011). Conventional orthogonal (coronal, sagittal, and horizontal) planes of the volumetric datasets were viewed simultaneously during segmentation of anatomical regions and tracts. Multiple semi-transparent image layers were used for comparing image features apparent in different modalities (Figure 2; see also Paper I, Fig. 1). Surface reconstructions of the segmented brain regions, presented in an interactive 3D view, aided refinement and validation of the delineations with regard to continuity, smoothness, and form and extent in three dimensions.

In high-contrast regions, the intensity-based region competition snake evolution algorithm implemented in ITK-SNAP was used to generate the core segmentation volume. The process was initialized by placing seeds in the region to be segmented and adjusting parameters that control feature image generation and snake propagation velocities. Snake evolution was then followed stepwise until an optimal segmentation was reached, characterized by having most of the selected region covered without extensive leakage to other areas. This method was applied to

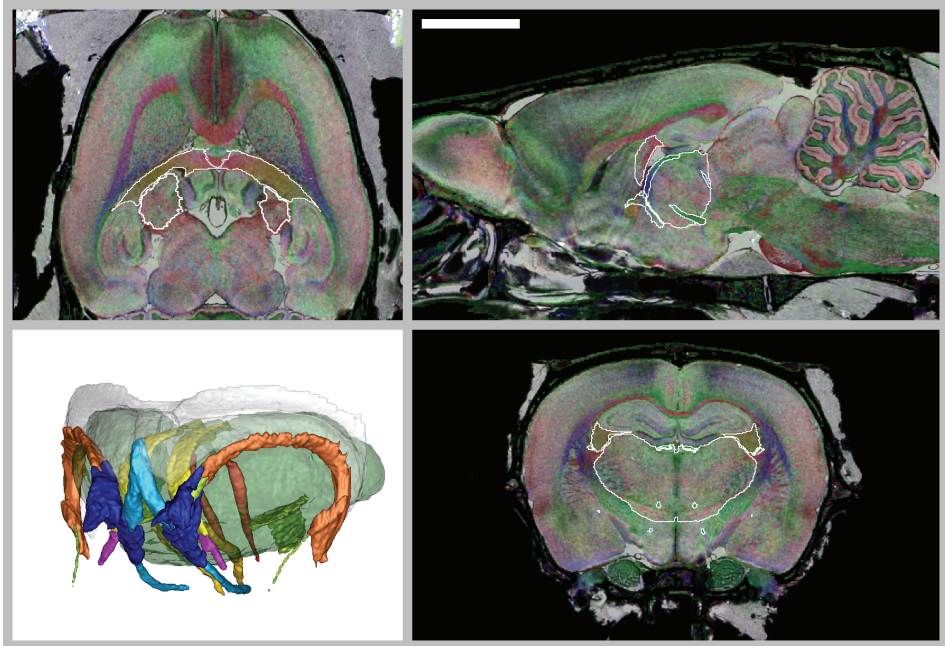


**Figure 2** | Volumetric segmentation environment in ITK-SNAP. Orthogonal views of the rat Waxholm Space template showing DTI as a semi-transparent overlay over  $T_2^*$ -weighted MRI. Delineations are displayed as an additional layer, here indicated only by outlines. Segmentation integrity is controlled using the 3D view, in this example showing the thalamus (green) and adjacent fiber tracts, including the fimbria (white), the fornix (cyan), the stria terminalis (orange) with its bed nucleus (dark blue), the stria medullaris (yellow) with its nucleus (magenta), and the fasciculus retroflexus (red). Scale bar: 5 mm

major white matter structures such as the corpus callosum, the anterior and posterior commissures, the corticofugal pathways, and the optic tract, as well as the ventricular system and the inner ear. For brain regions and tracts not suited for automatic segmentation, and for correcting the automatically generated core segmentations, manual two-dimensional and three-dimensional brush tools were used with different shapes (square, cube; circle, sphere) and diameters. We applied windowing fine-tuned to image intensity in each anatomical region to be able to make full use of the high dynamic range of the  $T_2^*$ -weighted MRI dataset that features over 10 million different intensity values in the subset containing the brain alone. Segmentations were saved in a single volumetric image file in standard Neuroimaging Informatics Technology Initiative format (NIfTI, .nii, <http://nifti.nimh.nih.gov/nifti-1/>) along with a text file (.label) storing the name, color, and transparency settings for each segmented region.

## **Anatomical delineations**

Parcellations in the atlas are based exclusively on image contrast in the high quality anatomical image volumes. We avoided adding boundaries without directly corresponding borders visible in the images, with a few appropriately documented exceptions for closing regions, and arbitrary straight-line cuts for delimiting structures with a gradual transition towards surrounding areas such as the olfactory bulb, the spinal trigeminal nuclei, or the cerebellar peduncles. We recorded and shared detailed delineation criteria for all anatomical structures.

When delineating the brain, we included the entire brain from the olfactory bulbs to the medulla oblongata (brainstem), aiming at a balanced distribution of the size and amount of anatomical structures throughout the brain (Figure 3). Given the high white matter to gray matter contrast in the volumetric images, we used major white matter tracts as the primary landmarks during the segmentation process. The high resolution DTI color maps made it possible to outline a total of 32 fiber bundles. Primary eigenvector orientations from the DTI maps were

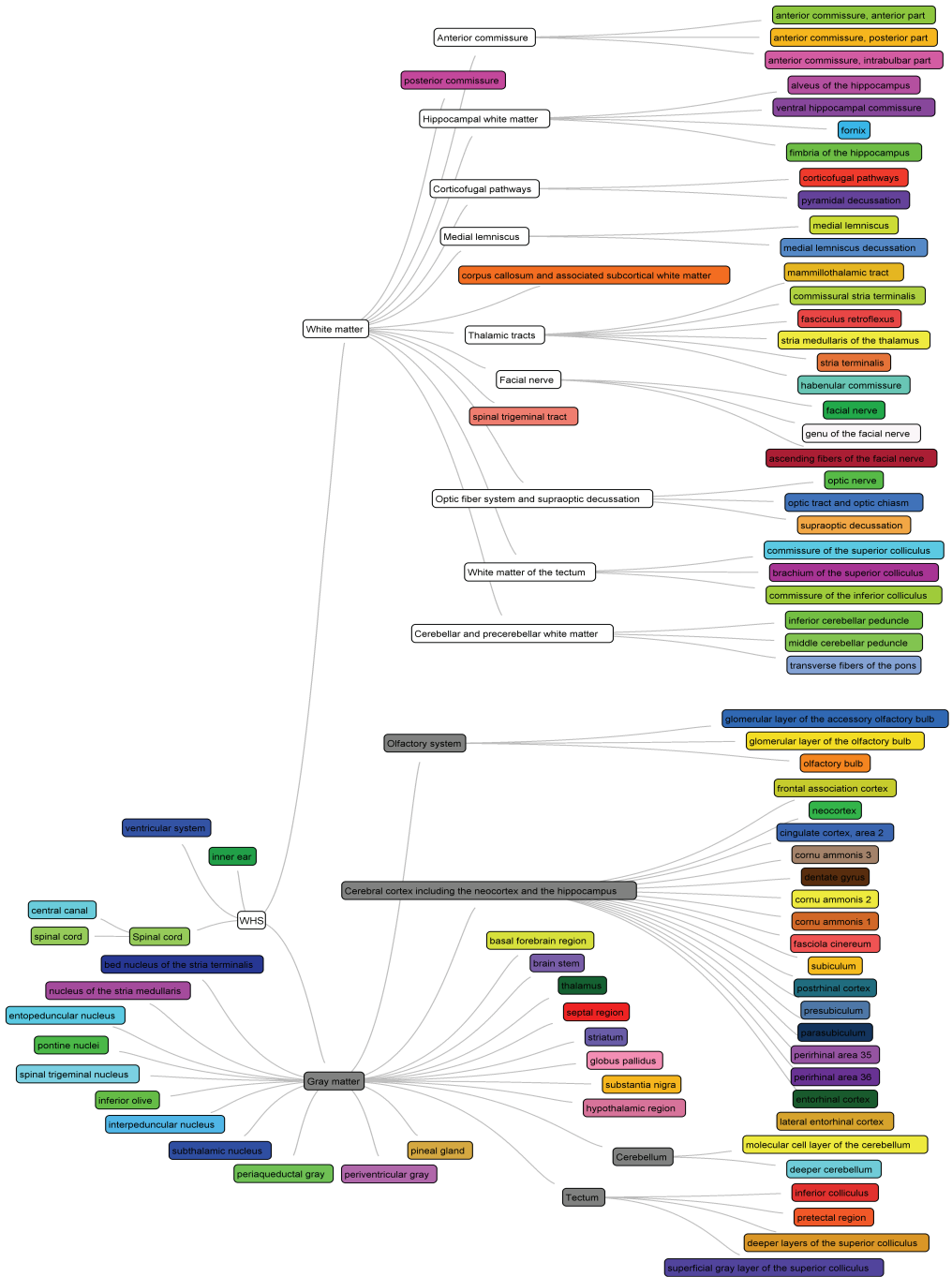


**Figure 3** | Basic hierarchy of the delineated anatomical regions and tracts (Paper I, atlas version 2) for use with the Mouse BIRN Atlasing Toolkit (MBAT) and PMOD

interpreted based on fiber directionality observed in corresponding myelin-stained sections. Boundaries between gray matter regions were delineated based on smaller, often subtle differences in MRI signal intensity corresponding to variations in cell density as observed in Nissl stained sections from matching regions. Delineations were aided by the most widely used rat brain atlases: the Paxinos and Watson (2007) atlas of the Wistar strain, and the Swanson (2004) atlas of the Sprague Dawley strain. Nomenclature was adopted from Paxinos and Watson, 2007.

To maximize the utility of the atlas, we did not limit delineations strictly to the brain. Additional structures include some of the cranial nerves: the optic nerve (II) up to the retina, the trigeminal nerve (V) towards the face, and the facial nerve (VII) from its point of entry to the brainstem; as well as the inner ear, and the upper segment of the spinal cord including the central canal and the surrounding periventricular gray.

### **Waxholm Space coordinate system for the rat brain**

Based on the white matter contrast in the  $T_2^*$ -weighted MRI and the fractional anisotropy image, we delineated the anterior and the posterior parts of the anterior commissure and identified its decussation. We located the Waxholm Space origin at the intersection of the mid-sagittal plane, a coronal plane passing midway (rostro-caudal) through the decussation of the anterior commissure, and a horizontal plane passing midway through the most dorsal and ventral aspects of the decussation. The initial version (v1) of the atlas was shared with all volumetric files in the acquisition orientation of the MRI template (anterior-left-superior; ALS). In addition to the original files being made available for reference, an updated version of the atlas (v1.01) was released with all volumes transformed into right-anterior-superior (RAS) orientation to ensure full compatibility with the NIfTI-1 standard. The changes were indicated in an Addendum to the original paper (Paper I). We recorded the voxel coordinates of the WHS origin (v1.01), and set up the internal coordinate system in each image volume in Waxholm Space.

We identified the coronal, sagittal, and lambdoid cranial sutures in the T<sub>2</sub>-weighted MRI (bo image) using windowing, and we recorded the position of bregma and lambda in voxel coordinates (Figure 4). We determined the location of lambda by first segmenting the dorsomedial half of the lambdoid suture on both sides, and then locating the midpoint of the curve of best fit along the suture in top view (Paxinos and Watson, 1982). Based on these 3D coordinates, we calculated the deviation of the acquisition angle of the atlasing template from the stereotaxic flat skull position in which bregma and lambda would fit in the same horizontal MRI slice (Paxinos and Watson, 1982).

We used bregma as the common reference point between the Waxholm Space atlas of the Sprague Dawley rat brain and the stereotaxic atlas of Paxinos and Watson (2007) to define an affine transformation from WHS to stereotaxic space (Paper III). We measured the anteroposterior distance between bregma and lambda in the two atlases to determine a uniform scaling factor (1.057) between the two coordinate systems, and we applied the previously calculated rotation between the two brains (-4.085° around the mediolateral axis). Coordinates transformed to stereotaxic space are interpreted in a right-anterior-superior (RAS) oriented coordinate system, representing 1) mediolateral distance from the midline where positive values are assigned to the right side, 2) anteroposterior distance from bregma; and 3) dorsoventral distance from bregma where negative values are assigned to coordinates ventral to bregma.

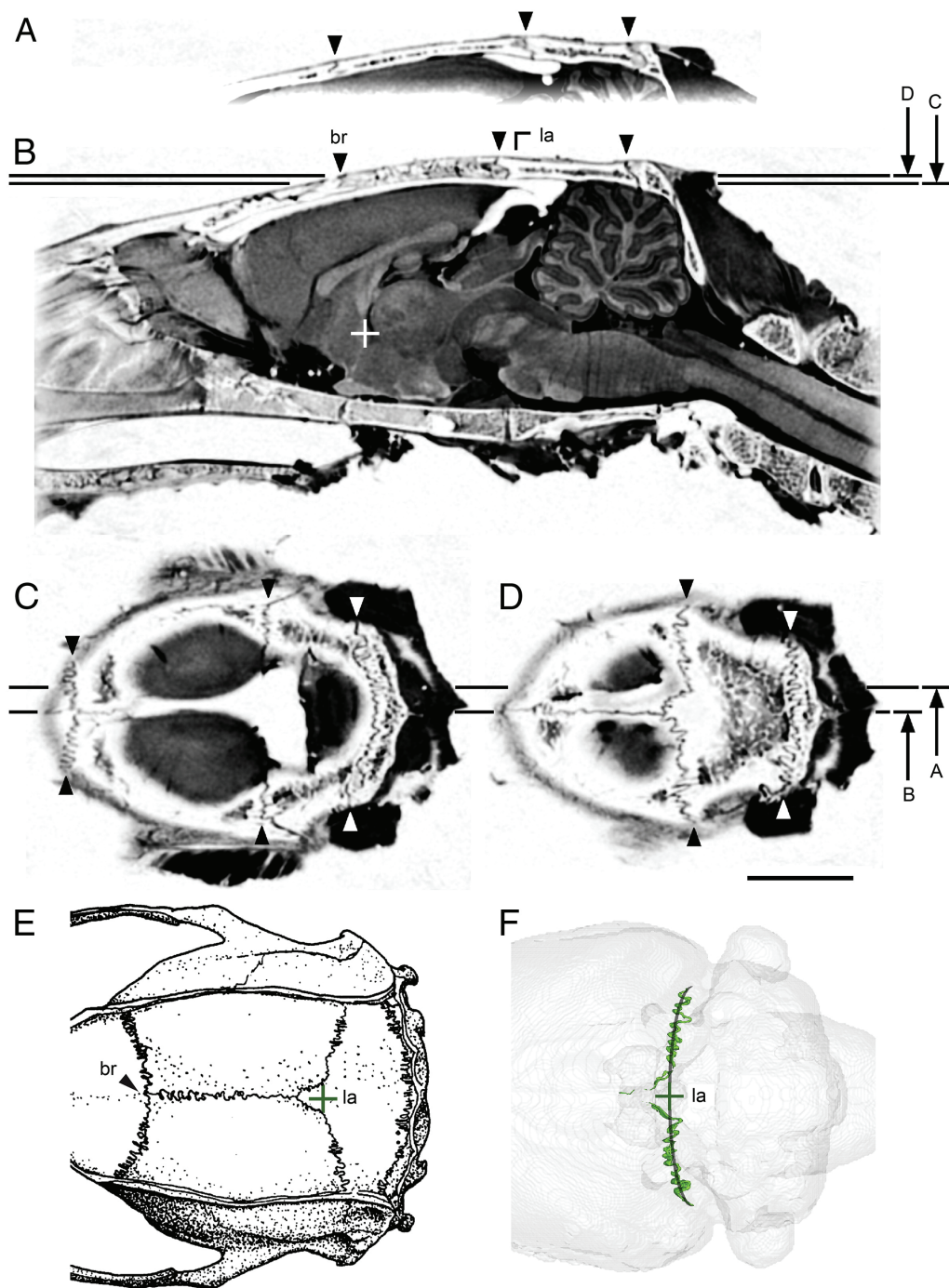


**Figure 4** | Cranial sutures and stereotaxic landmarks identified in the Waxholm Space MRI template for the rat brain (Paper I). WHS origin (white cross), bregma (br), lambda (la). Scale bar: 5 mm

## **Anatomical landmarks for image registration**

We applied the following selection procedure to establish a standardized set of anatomical landmarks that facilitate registration of whole-brain experimental image data showing variable levels of anatomical detail to volumetric reference material such as the Waxholm Space atlases of the mouse and rat brain (Paper II).

In search of distinct anatomical features in the brain and the ventricular system easily recognizable across image modalities, we identified an initial set of 50 landmark points in  $T_2$ -weighted anatomical MRI of a mouse brain (Erlangen template, see Table 1). The initial landmarks were evenly distributed throughout the brain, and visible in coronal slices of both  $T_1$ ,  $T_2$ , and  $T_2^*$ -weighted MRI. We created illustrated guidelines describing the visual characteristics of landmark locations avoiding extensive anatomical terminology. A test panel of 15 independent volunteers with (7) and without (8) basic knowledge of mouse brain anatomy located each landmark based on these guidelines in  $T_1$ ,  $T_2$ , and  $T_2^*$ -weighted MRI of two mouse brains. Landmark coordinates were recorded for all three contrasts, and the mean and standard deviation of the coordinates were calculated for each landmark. Landmarks with coronal in-plane coordinates showing a maximum standard deviation of 1.5 voxels (130.5  $\mu\text{m}$ ) were selected and further analyzed for identification reliability considering localization accuracy and probability of successful identification across test panel members. Additional image material from rats and mice was used to assess the usability of the selected landmarks in modalities other than MRI.

The sixteen landmarks that fit the above selection criteria were used for testing the accuracy of landmark-based registration between one of the  $T_1$ -weighted Erlangen datasets and the  $T_2^*$ -weighted MRI of the Waxholm mouse template. Images with different contrasts, different acquisition angles ( $23.5^\circ$ ), and different resolutions (87  $\mu\text{m}$  and 21  $\mu\text{m}$ ) were deliberately chosen to simulate a realistic scenario. We measured the average distance between corresponding landmarks in the two volumes following affine registration based on the selected landmarks.



We co-registered microscopic resolution computed tomography ( $\mu$ CT) and T<sub>2</sub>-weighted MRI of the heads of four mice to evaluate the variability of the anteroposterior position of bregma and the lambdoid junction relative to underlying brain anatomy. Following alignment, we identified the stereotaxic atlas plate (Franklin and Paxinos, 2008) corresponding to the coronal MRI slice at each cranial landmark, and we measured the anteroposterior distance to the respective landmark in the atlas. Finally, we compared the variability of the measurement results to that of the previously acquired soft-tissue landmark coordinates along the same axis.

### **Detection and spatial alignment of neuronal labeling**

With the aim to demonstrate the use of newly developed volumetric atlases in spatial analysis of large 2D datasets encompassing the whole brain, we designed a workflow that facilitates assignment of anatomical location to brain-wide axonal tract-tracing data. We developed image processing modules that automate the detection and quantification of labeled neurons in series of section images, and an alignment module that enables fast and flexible registration to volumetric datasets, and acquisition of coordinates in 3D atlas space.

We created new plugins and macros for the open source image processing software ImageJ (<http://imagej.nih.gov/ij/>) for the detection and measurement of BDA and *Pha*-L labeling in microscopic image series of the rat brain (Paper III). The new modules produce maps of labeled neuronal axons and cell bodies in the images, and provide tools for quantification of the amount and position of labeling.

Labeling detection is implemented in two main steps. First, original color (RGB) images from microscopy are converted to grayscale according to the type of labeling and counterstain. We acquired optical density vectors for the color deconvolution method described by Ruifrok and Johnston (2001) for multiple combinations of labeling and background (BDA, BDA combined with Neutral Red, *Pha*-L, *Pha*-L combined with thionine, and BDA combined with cytochrome oxidase).

We optimized the Colour Deconvolution plugin for ImageJ by G. Landini (<http://www.mecourse.com/landinig/software/cdeconv/cdeconv.html>) for automation so that vectors are stored in a parameter file and grayscale images of the detected labeling are generated directly to the primary output channel without calculating the two other channels. In the second processing phase, grayscale images are thresholded using the IsoData algorithm and the resulting binary images are optionally further processed for noise reduction using a standard median filter. We implemented a new plugin for automatic measurement of labeled area, and automated particle analysis functionality in ImageJ to enable calculation of centroid position for labeled regions of interest. We created macros to automate the above processing steps for series of images. An optimal processing route and parameters determined based on images representative of the series can thus be applied automatically to all images without the need for user interaction. Measurement results are saved in a spreadsheet compatible format.

To assign anatomical location to labeling detected by the image processing modules, we developed a workflow module for alignment of section images to a volumetric atlas. Building on the isotropic properties of the Waxholm Space templates for the mouse and rat brain, the alignment module generates arbitrarily positioned, sized and oriented rectangular slices of the structural MRI and the associated anatomical delineations. Section images with cytoarchitectural counterstaining and corresponding labeling maps are co-visualized with custom-generated atlas slices in an interactive session, allowing the user to set the clip region and perform affine transformations to match the atlas slice to the section image.

Image alignment is an iterative process based on anatomical features visible in both images. First, an approximate anteroposterior position is determined, and the height, width, and in-plane rotation of the MRI slice is adjusted to fit the section image. Next, the slicing angle and the anteroposterior position of the slice is adjusted to match the section image. Optionally, the slice is moved in-plane to allow fine alignment of selected regions of interest in the section to corresponding regions in the

volumetric atlas. Finally, Waxholm Space coordinates are recorded for labeled elements of interest using an active cursor functionality. To facilitate registration of series containing hundreds of section images, alignment parameters are interpolated between 5-10 manually anchored sections spread throughout the series, and a provisional alignment is applied to intermediate sections. Manual adjustments complete the procedure for the full series.

## **Data sharing and documentation**

We share the main results of this work open access under, in most cases, a Creative Commons Attribution-NonCommercial-ShareAlike license (CC-BY-NC-SA, <http://creativecommons.org/licenses/by-nc-sa/4.0/>).

The Waxholm Space atlas of the Sprague Dawley rat brain (Paper I), including the MRI/DTI volumes of the atlas template, the raw diffusion tensor data, the anatomical delineations, masks for the complete brain volume and white and gray matter, and accompanying documentation is hosted at the Neuroimaging Informatics Tools and Resources Clearinghouse (NITRC, <http://www.nitrc.org/projects/whs-sd-atlas>). All volumetric files are provided in standard gzipped NIfTI (.nii.gz) format. Labels identifying the names of anatomical regions and tracts delineated in the atlas are shared in formats compatible with ITK-SNAP (.label), MBAT (.ilf) and PMOD/PNEURO (.txt, .manifest). For use with the Mouse BIRN Atlas Tool, we built a basic hierarchy of the delineated structures (Figure 3) and set up the necessary XML-based configuration files (.atlas) for each version of the atlas (v1, v1.01, v2). The same hierarchy is displayed by the PMOD label (v2). Along with the atlas, we provide an overview of available atlas files and their usage, release notes for each atlas version, graphical illustrations of the orientation of the Waxholm Space coordinate system, and guidelines for coordinate calculations across reference systems and atlas versions (see Appendix).

An interactive list of the anatomical landmarks proposed for image registration (Paper II) is shared through the Scalable Brain Atlas (<http://scalablebrainatlas.incf.org>), including coordinates in mouse and rat Waxholm Space, and a simple visualization of their 3D position within the brain. Landmark positions are also marked in a browser-friendly version of both the C57BL/6J mouse ( $T_1$ ,  $T_2$ , and  $T_2^*$ -weighted MRI) and the Sprague Dawley rat WHS template ( $T_2^*$ -weighted MRI). We provide an illustrated guide for locating each landmark in coronal image series of the mouse and rat brain.

Image processing modules for automatic detection of labeling in series of microscopic section images (Paper III) are available open source on the ImageJ Documentation Wiki ([http://imagejdocu.tudor.lu/doku.php?id=plugin:analysis:autodetection\\_of\\_neuronal\\_labeling\\_in\\_histological\\_image\\_series:start](http://imagejdocu.tudor.lu/doku.php?id=plugin:analysis:autodetection_of_neuronal_labeling_in_histological_image_series:start)), accompanied by a summary of the functionality of each module and instructions for usage. A stand-alone version of the alignment module connecting microscopic section images to volumetric atlases is shared on NITRC (<http://www.nitrc.org/projects/cutnii>).

# **RESULTS**

**SUMMARY OF PAPERS I-III.**



# PAPER I.

## Waxholm Space atlas of the Sprague Dawley rat brain

*Papp EA, Leergaard TB, Calabrese E, Johnson GA, Bjaalie JG*  
*NeuroImage 97 (2014) 374-386. DOI: [10.1016/j.neuroimage.2014.04.001](https://doi.org/10.1016/j.neuroimage.2014.04.001)*  
*NeuroImage 105 (2015) 561-562. DOI: [10.1016/j.neuroimage.2014.10.017](https://doi.org/10.1016/j.neuroimage.2014.10.017)*

Essential elements for building an atlas of brain anatomy include high quality biological reference material, a comprehensive set of anatomical maps based on well-documented observations in this reference material, and an unambiguously defined spatial reference system for navigation in the atlas and in aligned anatomical datasets. We present an atlas of the adult Sprague Dawley rat brain designed along these principles. We used state-of-the-art non-distorted volumetric image material to build 3D anatomical delineations of the whole brain. The atlas is navigated using a novel coordinate system based on internal brain landmarks (Waxholm Space, WHS) interoperable with the stereotaxic system.

We acquired microscopic resolution contrast-enhanced *ex vivo* MRI and DTI from the brain of an adult male Sprague Dawley rat. The volumetric images consisting of 39  $\mu\text{m}$  and 78  $\mu\text{m}$  voxels provide the highest resolution atlasing template currently available for this strain. Imaging was performed with the brain residing intact in the skull to minimize distortions. Isotropic acquisition of the datasets allows custom-angle slicing with minimal loss of image quality from interpolation.

Based on image contrast in the MRI and DTI volumes, we created the first comprehensive volumetric atlas for the Sprague Dawley rat brain. We identified primary landmarks and boundaries visible in the microscopic resolution magnetic resonance images, and delineated 76 major anatomical regions, tracts, and nuclei in three dimensions. The atlas covers the entire brain from the olfactory bulbs to the upper spinal cord, outlined individually for each hemisphere. Delineation criteria are described in detail for all regions.

To provide spatial reference in the atlas template, we applied the Waxholm Space standard in the rat brain for the first time. We identified and documented the position of the WHS origin relative to the anterior commissure, and defined the orientation of the coordinate system axes. With the aim to connect the atlas to the widely used stereotaxic coordinate space, we located major cranial landmarks bregma and lambda and measured their WHS coordinates.

The atlas is available open access through the Neuroimaging Informatics Tools and Resources Clearinghouse (NITRC) in standard neuroimaging (NIfTI) format. The image headers incorporate the position of the WHS origin, allowing real-time recording of metric WHS coordinates for any point of interest in the atlas. We share guidelines on the use of the atlas template and the WHS coordinate system with a perspective towards modular expansion of the atlas and connection to initiatives for multi-modal anatomical data integration.



## PAPER II.

### **Anatomical landmarks for registration of experimental image data to volumetric rodent brain atlasing templates**

*Sergejeva M, Papp EA, Bakker R, Gaudnek A, Okamura-Oho Y, Boline J, Bjaalie JG, Hess A. Journal of Neuroscience Methods 240 (2015) 161-169.*

*DOI: [10.1016/j.jneumeth.2014.11.005](https://doi.org/10.1016/j.jneumeth.2014.11.005)*

Assignment of anatomical location to the diversity of image material acquired from the rodent brain plays a central role in building an integrative atlasing environment. Recently developed open access atlases based on non-distorted isotropic MRI have the potential to connect experimental images from different modalities with variable levels of structural detail. Aiming to facilitate landmark-based registration of whole-brain image datasets to the Waxholm Space atlasing templates, we established a standardized set of anatomical landmarks in the mouse and rat brain.

Based on quantitative testing of potential landmark points recognizable in  $T_1$ ,  $T_2$ , and  $T_2^*$ -weighted MRI of the adult C57BL/6J mouse brain, we concluded on 16 landmarks that were consistently identified across assessors regardless of their level of anatomical experience with a spatial accuracy of 1.5 voxels (130.5  $\mu\text{m}$ ) and an average identification probability of 98%. We found that 14 of these landmarks were applicable to  $T_2^*$ -weighted MRI of the rat brain. We used coronal image series of Nissl-stained histological sections from the mouse and rat brain, and unstained block-face images from the mouse brain to assess whether the landmarks are recognizable in modalities other than MRI. All 16 landmarks were identifiable, though less distinct, in all mouse brain images. In the rat brain microscopy material, all but one of the landmarks previously identified in MRI were visible.

We located all landmarks in  $T_1$ ,  $T_2$ , and  $T_2^*$ -weighted MRI from the mouse brain WHS template, and landmarks applicable to the rat brain in  $T_2^*$ -weighted MRI from the Sprague Dawley rat WHS template. Waxholm Space coordinates for each landmark position are shared via the web-based Scalable Brain Atlas (<http://scalablebrainatlas.incf.org>). In addition, we share illustrated guides for locating the landmarks in anatomical images, including both example pictures and a description free from extensive anatomical terminology.

We measured the level of registration accuracy attainable using the standardized landmark set across  $T_1$  and  $T_2^*$ -weighted MRI of the mouse brain acquired in different angles and resolution. The average distance between corresponding landmarks in the two volumes following affine registration was  $134 \pm 20$   $\mu\text{m}$ , corresponding to ca. 1.5 voxels in the source image. Based on co-registered  $\mu\text{CT}$  and  $T_2$ -weighted MRI acquired from four mice, we evaluated whether cranial landmarks provide refining options for brain-to-brain registration between volumetric datasets. We concluded that internal brain landmarks, if available, enable higher registration precision.

## PAPER III.

### **Brain-wide mapping of axonal connections: workflow for automated detection and spatial analysis of labeling in microscopic sections**

*Papp EA, Leergaard TB, Csucs G, Bjaalie JG*

*Frontiers in Neuroinformatics (2016) 10:11*

DOI: [10.3389/fninf.2016.00011](https://doi.org/10.3389/fninf.2016.00011)

Building a comprehensive map of the structural organization of neuronal pathways across the brain requires systematic mapping of connections between individual regions and integration of the resulting anatomical information in a common spatial framework. Axonal tracing techniques facilitate brain-wide measurement of the extent and location of neuronal labeling using microscopic image series of histological sections. MRI-based atlases offer non-distorted anatomical reference for spatial integration of the resulting image data. In this paper, we present a workflow that efficiently connects complete tract-tracing datasets from the rodent brain to volumetric reference atlases through automated image processing and alignment steps.

Manual methods for recording axonal labeling in large image series are tedious and difficult to standardize. We have automated labeling detection in histological section images by creating image processing modules for the NIH ImageJ software. The new modules allow automatic processing of brain-wide image series following an optimal processing route determined based on a set of representative images. Axonal labeling of biotinylated dextran amine (BDA) and *Phaseolus vulgaris* leucoagglutinin (*Pha-L*) is detected against different cytoarchitectural counterstains, and plotted on binary labeling maps. Automatic measurements are provided for recording labeled area throughout the image series and for calculating the centroid position of injection sites, larger plexuses, and terminal fields.

We evaluated the effectiveness of the automatic labeling detection modules using high-resolution microscopic image series from axonal tracing experiments in which different parts of the rat primary somatosensory cortex had been injected with BDA or *Pha-L*. While automated image processing was found to be less sensitive to incompletely or weakly stained solitary fibers (low amounts of labeling), in areas containing modest to high amounts of labeling, the automatic method provided results comparable to rigorous manual analysis of the same material (Zakiewicz et al. 2014).

To assign anatomical location to the detected labeling, we developed an alignment module that generates customized atlas plates from a selected volumetric template that match the dimensions and slicing angle of the histological section series. Cytoarchitectural contrast in the sections is used in combination with the binary labeling maps to assign anatomical location to the detected labeling in 3D brain atlas space. Alignment of large series of images is supported by propagation of parameters across the series based on a few key images aligned manually. We demonstrate the use of the Waxholm Space (WHS) atlas of the Sprague Dawley rat brain for determining the position of sections from the above material within the brain and assigning atlas coordinates to detected labeling. WHS coordinates are transformed to stereotaxic coordinates for access to additional parcellation information and comparison to legacy data.

Integration of the large amounts of image data acquired from the brain by tract-tracing studies is essential for synthesizing new knowledge about how the brain is wired. Our workflow modules increase the efficiency and reliability of recording the presence, amount, and localization of labeling in large microscopy datasets. Further, our results show how recently introduced volumetric reference atlases such as the Waxholm Space atlas of the Sprague Dawley rat brain can be combined with stereotaxic atlases for spatial analysis across 2D and 3D anatomical reference material.

## DISCUSSION

The ambition of this study is to advance digital atlasing of the rodent brain towards a new generation of volumetric atlases that facilitate integration of whole-brain image data from multiple modalities. Developments in high resolution soft tissue imaging have led to a rapid expansion of image data mapping the entire brains of rats and mice. Assembling anatomical information across 3D image volumes and comprehensive microscopic image series requires a new type of spatial reference and corresponding atlasing resources. We identified four key elements for atlas-based integration of 2D and 3D brain images: 1) a spatial reference system defined by landmarks within the brain, 2) high quality anatomical reference material revealing these landmarks, 3) methodology and tools for image alignment and analysis, and 4) open access to both methods, data and software.

We have contributed to this vision by creating a volumetric atlas of the Sprague Dawley rat brain, implementing the Waxholm Space standard in this atlas, and publicly sharing both the high quality atlasing template and the corresponding brain-wide anatomical delineations. We provide extensive documentation on the delineation criteria, as well as practical guidelines for using the atlas and the WHS coordinate system. To support anchoring of experimental image data to Waxholm Space, we defined a standardized set of anatomical landmarks reliably identified in multiple image modalities, and designed a workflow for processing, alignment, and spatial analysis of image series using the new atlas. In the following chapter, we evaluate the individual results of this work and its implications on digital atlasing.

## **Anatomical reference material**

Integration of images from across the brain into a common anatomical space requires a reference atlas that represents the entire brain with high anatomical fidelity close to the *in vivo* situation. For mapping diverse types of measurements to this reference space, the atlas needs to display detailed structural contrast of major brain regions with a comprehensive set of anatomical boundaries identified. Tomographic imaging, and in particular magnetic resonance imaging is uniquely suited to produce such anatomical reference material. We used contrast-enhanced MR microscopy (Badea et al. 2007) complemented by fiber directionality maps from diffusion tensor imaging for delineation of regions and tracts throughout the Sprague Dawley rat brain (Paper I). The quality of the images is well exemplified by the visibility of fine anatomical details such as individual cell layers in the cerebral and cerebellar cortex and the hippocampus, as well as thin white matter sheets in the inferior external capsule and the supraoptic decussation. The completeness of the material, the high spatial resolution of the MRI, and the availability of multiple image contrasts allowed us to locate several anatomical features useful for alignment of experimental images to the atlas. Notably, cranial sutures and related stereotaxic landmarks bregma and lambda are also recognizable in the MRI, attributed to the presence of contrast agent in the connective tissue between the bone plates of the skull.

In order to achieve the best possible image quality and avoid motion or pulsation artifacts, the MRI was acquired *ex vivo* with the brain residing intact in the cranium. It has been shown that excision of the brain from the skull results in shape distortions (Ma et al. 2005) compared to the *in vivo* state (Ma et al. 2008), whereas *in situ* imaging does not alter brain morphology (Oguz et al. 2013). Imaging postmortem tissue allowed for long scan sessions at a high field strength (7T), resulting in highly increased signal to noise ratio and significantly improved image quality over *in vivo* imaging. Consecutive acquisition of different MRI contrasts yielded inherently co-registered images, eliminating errors from image registration between scans. Perfusion with a paramagnetic agent during fixation further enhanced contrast throughout the material (Huang et al.

2009). With regard to the diffusion-weighted images, it should be noted that the diffusion properties of formalin-fixed brain tissue are altered from the *in vivo* situation, but diffusion anisotropy, on the basis of which fiber orientations were interpreted, is preserved (d'Arceuil and de Crespigny, 2007; Sun et al. 2003).

While the non-invasive nature of the imaging process makes MRI and DTI powerful tools for establishing a morphologically correct reference atlas, the depth of anatomical mapping achievable using this type of material has its technical and methodological limits. The minimal diameter of structural features that can be outlined in digital image volumes is in principle determined by the voxel size. Image intensity in each voxel represents an average of the magnetic susceptibility or fractional anisotropy measured in the corresponding tissue volume, blending together values from subvoxel-sized tissue elements. This phenomenon, known as the partial volume effect, makes the delineation of fine details at the single voxel scale prone to error. Similarly, in DTI measurements from regions with crossing fibers, the individual fiber orientations may be obfuscated by averaging. In our image material, this effect is reinforced by the double voxel size of the DTI (78 $\mu$ m) compared to the MRI (39 $\mu$ m). To compensate for these restrictions, we focused our efforts on major brain regions and tracts of relatively larger volume, and we used microscopic image material of cellular and myelin stains from comparable animals to aid delineation decisions.

The atlas template proposed in Paper I depicts the brain anatomy of a single animal, without smoothing or mirroring of either side. A Sprague Dawley specimen was chosen as there was no comprehensive volumetric atlas for this strain previously available. The weight, age and sex of the animal is representative to common laboratory practice. Compared to widely used stereotaxic atlases for the rat (Paxinos and Watson, 2007; Swanson, 2004), the weight of our animal is ca. 24% larger, although very close to the average weight of an adult male Sprague Dawley (see [criver.com](http://criver.com)). Since the present atlas is only valid for adult animals, additional atlases are needed to cover the newborn, young, adolescent and aging rat brain (see e.g. Calabrese et al. 2013). The use of male rats is

clearly overrepresented in currently available atlas resources, our atlas included. The transition to open atlas resources will likely help balance the situation by facilitating community data sharing.

As pointed out by Arthur W. Toga, “The success of any brain atlas depends on how well the anatomies of individual subjects match the anatomy in the atlas” (Toga, 2002). An essential next step to make our atlas more representative therefore should be to include anatomical information from several additional animals to build a population-based template. Co-registration of series of structural image volumes and adaptation of the original anatomical delineations to the individual brains then allows probabilistic mapping of specific brain regions. Creating a gold standard segmentation by careful manual delineation of a complete set of brain regions and tracts on the basis of a single high quality anatomical image forms a prerequisite to such developments (Badea et al. 2009), since population averaging significantly blurs the template, hampering precise definition of borders. The gold standard labeled volume we created for the Sprague Dawley rat brain thus provides a basis for atlas-based segmentation of additional volumetric datasets using automated methods (Ali et al. 2005; Bello et al. 2007; Cabezas et al. 2011; Niedworok et al. 2016).



## **Delineations of white and gray matter**

On the basis of image contrast in the high fidelity anatomical template, we were able to delineate 76 major regions and tracts of the rat brain in three dimensions. Segmentations were carried out *de novo* by a single investigator to ensure consistency and avoid possible bias that the re-use of volumetric or section-based maps from external sources could have introduced. While most of the subdivisions were created manually, we also explored to what extent automatic methods can be used for outlining brain regions in MRI without *a priori* anatomical information. Although only effective in a limited number of cases, automatic segmentation considerably sped up the delineation of high-contrast structures by generating the core segmentation volume.

The volumetric format of the anatomical images we built the atlas on makes it possible to study the brain in its native 3D space. The MRI and DTI allow the viewer to observe brain regions and tracts from multiple angles simultaneously, and examine intersecting planes through a region of interest within the same brain. The level of morphological feedback obtained from such 3D analysis during the delineation process, together with the volumetric segmentation toolset provided by ITK-SNAP, enabled us to create robust and well-composed segmentations consistent across all three planes. The 3D nature of the atlas, best appreciated through surface models of the individual anatomical structures (Paper I, Fig. 6), promotes the understanding of spatial relationships between brain regions, tracts, and experimental data mapped onto the atlas.

In contrast with idealized anatomical drawings in classical book-format atlases, often presented as vector graphics, our volumetric atlas features one-to-one correspondence to the underlying MRI data. Each image voxel in the delineation volume is assigned a single anatomical label, thereby avoiding ambiguous annotation such as dotted lines, unlabeled areas, or unmarked transition zones between regions. While this format does not allow multiple anatomical interpretations in the same atlas file, open access to the atlas promotes the development and sharing of alternative or refined versions.

With the future perspective of atlas-based integration of diverse types of experimental image data across the brain, our ambition was to develop a comprehensive set of delineations with no uncharted areas and a close to homogenous distribution of anatomical parcellations in both white and gray matter. Owing to the high white to gray matter contrast in the MRI and the availability of fiber directionality maps (DTI), we achieved a relatively even distribution of white matter segmentations, from major tracts such as the corticofugal pathways and the corpus callosum to smaller fiber bundles such as the fasciculus retroflexus or the habenular commissure. The varying, often subtle MRI contrast within gray matter, however, made the determination of boundaries between cell-dense regions more difficult. Our segmentation efforts in these areas were guided by widely used histological atlases to ensure that the boundaries recorded based on MRI or DTI are in agreement with corresponding histologically defined boundaries (Paxinos and Watson, 2007; Swanson, 2004). In areas adjacent to fiber tracts, as in the case of individual nuclei e.g. the subthalamic nucleus, the bed nucleus of the stria terminalis, and the entopeduncular nucleus, as well as in regions showing a difference in the presence, density or orientation of traversing fibers, such as the striatum against the globus pallidus or the superior colliculus against the reticular formation, more detailed delineations were possible compared to other areas. This is especially apparent in the midbrain. In other parts of gray matter, most prominently in the cerebral cortex, the thalamus, the brainstem, the basal forebrain, and the hypothalamus, the granularity of the atlas is considerably lower.

To improve the level of segmentation detail in such regions, two main approaches are possible. First, careful observation of the current atlasing template aided by histological or other material revealing specific anatomical landmarks may allow direct identification of boundaries not yet indicated in the atlas. The first example for such expansion of the original delineation set is represented by the detailed subdivision of the hippocampal region by Kjonigsen et al. (2015), shared as version 2 of the atlas. Similar to previous methodology, subdivisions were based on MRI contrast guided by visual inspection of immunohistochemical material not spatially registered to the template (Kjonigsen et al. 2011). Further

atlasing efforts following the same principle are underway to create a 3D map of the rat auditory system (Imad et al. 2017; Osen et al. in preparation). Second, the limited resolution and specificity of the current atlasing template will necessitate the use of additional material for precise identification of anatomical boundaries within larger gray matter regions. In such cases, delineations may be created based on image features in other modalities (Augustinack et al. 2013), and transferred to the atlas by spatial registration of the new images to the template. Finally, the resolution of MRI is expected to further improve over the next decades towards enabling cellular mapping of neural tissue (Flint et al. 2009). Such developments shall be reflected in introducing new template versions and corresponding atlas updates.

Delineations presented in Paper I are not aiming to provide new interpretations of rat brain anatomy, depicted in far greater detail in stereotaxic atlases and relevant literature (for an overview, see Zilles, 2012). Rather, the main contribution of the new atlas lies in establishing morphologically correct anatomical reference for the Sprague Dawley strain in a volumetric format. The non-distorted isotropic MRI template serves as an ideal registration target for both 2D and 3D images, connecting more detailed atlasing material as well as experimental data to the atlas. The corresponding 3D anatomical delineations facilitate navigation across the brain and provide immediate access to volume of interest-based analysis for non-structural datasets aligned with the template. The resulting atlasing framework, when complemented by tools and workflows for image alignment and analysis, and equipped with a standardized coordinate space, makes it possible to integrate anatomical information from multiple modalities (Leergaard et al. 2014; Pawela et al. 2017; Schubert et al. 2016; Thomas et al. 2016).

## **Spatial reference: Waxholm Space for the rat brain**

Interoperability across atlas resources capturing the anatomy, gene expression, connectivity, development, or other aspects of the brain is a key requirement for data integration in neuroscience. In order to relate different types of information retrieved from these resources to each other and to newly acquired data, a common spatial reference system is needed. Waxholm Space has been designed to act as such a standard reference for anatomical location in the rodent brain. We present a practical implementation of the Waxholm Space standard for the Sprague Dawley rat (Paper I), including the placement and orientation of the WHS coordinate system relative to the accompanying anatomical template, and documentation and guidelines for its use with multiple atlas software. We anchored Waxholm Space to the stereotaxic space through locating standard cranial landmarks in WHS and defining an affine transformation between the two coordinate systems. Finally, we demonstrated the use of Waxholm Space in localization of signal within the brain and retrieving information on cytoarchitectonic boundaries at the same anatomical position from a stereotaxic atlas (Paper III).

In mathematical terms, a three-dimensional Cartesian coordinate system is defined by the spatial position of the origin, the direction of the axes, and the units to be used. The definition of the Waxholm Space coordinate system places the main emphasis on describing the anatomical position of the origin within the brain (Hawrylycz et al. 2011), while the units and the orientation of the axes are only implicitly given by the image headers of the mouse WHS template (Johnson et al. 2010). In support of the ambition to extend the standard to other rodent strains and species, we complemented previous documentation with 3D visual guidelines that illustrate the orientation of the coordinate axes (see Appendix) and the position of the WHS origin relative to the decussation of the anterior commissure (Paper I, Fig. 2). We set up the Waxholm Space coordinate system in the rat brain according to its implementation in the mouse. Thus, the position of the origin is anatomically identical in the two templates, and the coordinate axes run parallel to the slice planes of the MRI in both the mouse and the rat

WHS coordinate system. Due to a slight difference in the acquisition orientation of the two MRI datasets, the direction of the anteroposterior and inferosuperior coordinate axes shows a few degrees deviation between the two systems. Since new experimental data or other atlas resources are mapped to Waxholm Space based on anatomical features, and differences in the relative orientation of the images are encoded in the mathematical transformation between the individual coordinate systems (see Paper III), such variations do not affect the usability of the reference space.

Waxholm Space connects 2D and 3D experimental image data from the rodent brain to multiple atlas resources in a two-step process. First, pairwise coordinate transformations between each atlas resource and the WHS template are established based on anatomical image alignment (Zaslavsky et al. 2014). Once these mappings are in place, experimental datasets registered to Waxholm Space are able to query each resource for spatially indexed data based on the WHS coordinates of regions of interest (Baldock and Burger, 2012). For the newly introduced Waxholm Space atlas of the rat brain it is essential to ensure compatibility towards the most commonly used anatomical resource in rat brain research, the Paxinos and Watson atlas (Paxinos and Watson, 2007). Therefore the highest priority coordinate transformation to be determined is the mapping between WHS and the stereotaxic space. In Paper III, we calculated a preliminary transformation between the two systems based on common anatomical anchors identified in Paper I. Since the stereotaxic coordinate grid is equipped with multiple reference points and axes, we specified a right-anterior-superior (RAS) oriented stereotaxic coordinate system to facilitate univocal and reproducible mathematical mapping between the two spaces. Bregma was set as the origin for being a landmark identified in both atlases. Our choice of a right-handed coordinate system is in line with current neuroimaging practice (see e.g. the NIfTI-1 standard), though inferosuperior coordinates for structures within the brain are negative as a consequence of the origin located above the brain (Figure 1). As the anatomical basis for the coordinate transformation, we used cranial landmarks to perform a global affine alignment that matches the position, overall size, and

rotation of the skull in the two atlases. Having brought these stereotaxic parameters into alignment, we may expect the accuracy of the transformation to be below 0.3 mm (Paxinos et al. 1985). The main advantage of this approach is the simplicity of coordinate calculations between Waxholm Space and the stereotaxic space without a need for specific software. As illustrated by spatial analysis of axonal tracing material presented in Paper III (Fig. 5), the availability of this basic transformation makes it possible to combine the flexibility of section to volume alignment in WHS with immediate access to detailed anatomical parcellations in the Paxinos and Watson atlas.

The above mapping between Waxholm Space and the stereotaxic space provides a relatively crude starting point for integration of spatially related data across the two coordinate systems. Local discrepancies arising from histological distortions, or inter-individual or inter-strain differences in brain structure are not incorporated in the transformation, and thus may introduce significant localization error in some brain regions (Kötter and Wanke, 2005). To optimize mapping accuracy, detailed brain-to-brain alignment is needed. Considering that the anatomical maps in the Paxinos and Watson (2007) atlas do not form a continuous volume, the following alignment routes are available. The isotropic nature of the Waxholm Space template allows reslicing of the MRI based on visual matching of brain landmarks in the two atlases so that the principal axes of the MRI are aligned to the axes of the stereotaxic atlas. In rats from the Wistar strain, this method yielded comparable accuracy to our transformation (Johnson et al. 2012). Alternatively, a volumetric reconstruction built from the stereotaxic atlas plates may be registered to the WHS template on a volume-to-volume basis. In this case, accuracy will depend on the degrees of freedom provided by the reconstruction and registration algorithms. To maximize the level of alignment between the two atlases, each stereotaxic atlas plate needs to be individually aligned to the WHS template. Similar to the alignment example presented in Paper III, the process involves iterative steps of reslicing the MRI to match the angle of the stereotaxic sections, and affine or non-linear 2D to 2D alignment. The resulting transformation can be represented by a volumetric deformation field.

Waxholm Space is intended as a mediator between newly acquired data and existing knowledge about the brain through facilitating anatomical localization of findings and providing access to spatially related information stored in diverse atlases and databases. The realization of this concept requires that a variety of experimental data and atlas resources are mapped to WHS. As demonstrated by the emergence of multiple integrative resources over the last years, several areas of rat brain research could benefit from spatial interoperability, including the study of connectivity (Oh et al. 2014; Zakiewicz et al. 2011), gene expression (Shcherbatyy et al. 2015; Stansberg et al. 2011; Yu et al. 2014), and brain development (Calabrese et al. 2013; Khazipov et al. 2015; Rumpel et al. 2013). Connecting more atlas resources to Waxholm Space requires the contents of these resources to be spatially indexed according to WHS or a compatible coordinate space (e.g. the stereotaxic space). This may involve increasing the depth of spatial annotation from a semantic level to the level of coordinates, as well as managing metadata, and setting up software to handle incoming queries for spatial information, e.g. via web services. From the aspect of individual datasets, requirements include tools and workflows for image alignment and assignment of coordinates to data, software for building spatial queries towards atlas resources, and documentation and best practices that effectively lower the threshold to the steps involved. While the present project has provided key building blocks towards such developments, the multitude of demands for software, standards, and infrastructure for storage and shared access requires a coordinated effort from the neuroscience community. A promising initiative focusing on some of these challenges is represented by the Neuroinformatics Platform developed by the EU Human Brain Project (Amunts et al. 2016; <https://nip.humanbrainproject.eu>).

## **Connecting experimental image data to standard atlas space**

The introduction of new volumetric mouse and rat brain atlases that employ a non-stereotaxic reference system brings new approaches to the anatomical localization of findings in brain-wide image material. While the image-based nature of the new Waxholm Space reference atlases offers increased spatial precision compared to coordinate-based mapping, it also raises a challenge towards the alignment of images from diverse sources to MRI. In particular, tools and methods are needed for registration of 2D and 3D images with different or reduced anatomical contrast or resolution compared to the reference atlases, and for efficient alignment of large series of non-registered images from microscopy. With the aim to enable connecting different types of whole-brain image data to Waxholm Space, we defined standard anatomical landmarks in the mouse and rat brain for landmark-based registration across different levels of anatomical detail and resolution (Paper II). We demonstrated the flexibility of high resolution isotropic atlas volumes in section to volume alignment and spatial analysis of neuronal labeling. We combined series of automatic and semi-automatic steps for image acquisition, processing and alignment into a workflow to exemplify how traditional non-volumetric datasets can be efficiently connected to next-generation atlases (Paper III).

### ***Standard landmark set in Waxholm Space***

As a result of the rapid technological development over the last decades, a variety of imaging methods capturing the entire brain of rodents has become available. Common morphological features apparent in multiple image modalities showing different levels of anatomical detail offer a good starting point for image alignment to volumetric reference atlases. We established a set of standard anatomical landmarks in the mouse and rat brain based on the observation that in most magnetic resonance and histological images, major brain regions such as the cerebellum, the pons and the brainstem, the cortical hemispheres, the hippocampus, and the ventricular system, as well as major white matter tracts such as the corpus callosum and the anterior commissure can be distinguished. To



ensure full compatibility with the Waxholm Space atlases, we verified the reliability and spatial identification accuracy of each landmark in  $T_1$ ,  $T_2$ , and  $T_2^*$ -weighted MRI, and recorded their WHS coordinates. As expected, the visibility of the landmarks slightly varies across contrasts (Paper II, Table 2). From the proposed 16 landmarks in the mouse brain, at least 10 landmarks were characterized with a quality coefficient over 0.8 for each contrast, 10 were found highly reliable in two different contrasts, and 6 landmarks obtained a high reliability score in all three contrasts. These results, together with the accuracy obtained in our test case for landmark-based registration between  $T_1$  and  $T_2^*$ -weighted MRI, suggest that the landmark set is well suited for registration of images from all MRI contrasts towards the Waxholm Space templates.

Based on successful identification in microscopic image series of Nissl-stained sections and in unstained block-face images, we anticipate that most landmarks are also applicable in the alignment of images of serial sections co-registered into a volume, or histological image volumes collected using whole-brain light microscopic techniques such as serial two-photon tomography or light-sheet fluorescence microscopy. When working with coarsely reconstructed series, it should be noted that three landmarks defined based on the position of the cerebellum relative to the brainstem, and the distance between the posterior part of the cortical hemispheres, cannot be located accurately in images of free floating sections, since these spatial relations are lost during the cutting and mounting process. Two of these landmarks represent the hindmost elements of the landmark set, but as their anteroposterior position is not affected by the above uncertainty, they may be included in the alignment to reduce rotation errors between the source and target brains. It should also be considered that alignment accuracy will be limited by section thickness and spacing. For image series that are non-coregistered, incomplete, or that exhibit a large difference in acquisition angle compared to the conventional coronal plane, including sagittal or horizontal slices, a section-based approach is more appropriate (Paper III). Eventually, a coarse volumetric reconstruction may be combined with rigid or affine landmark-based registration methods to initialize a more accurate section-based alignment.

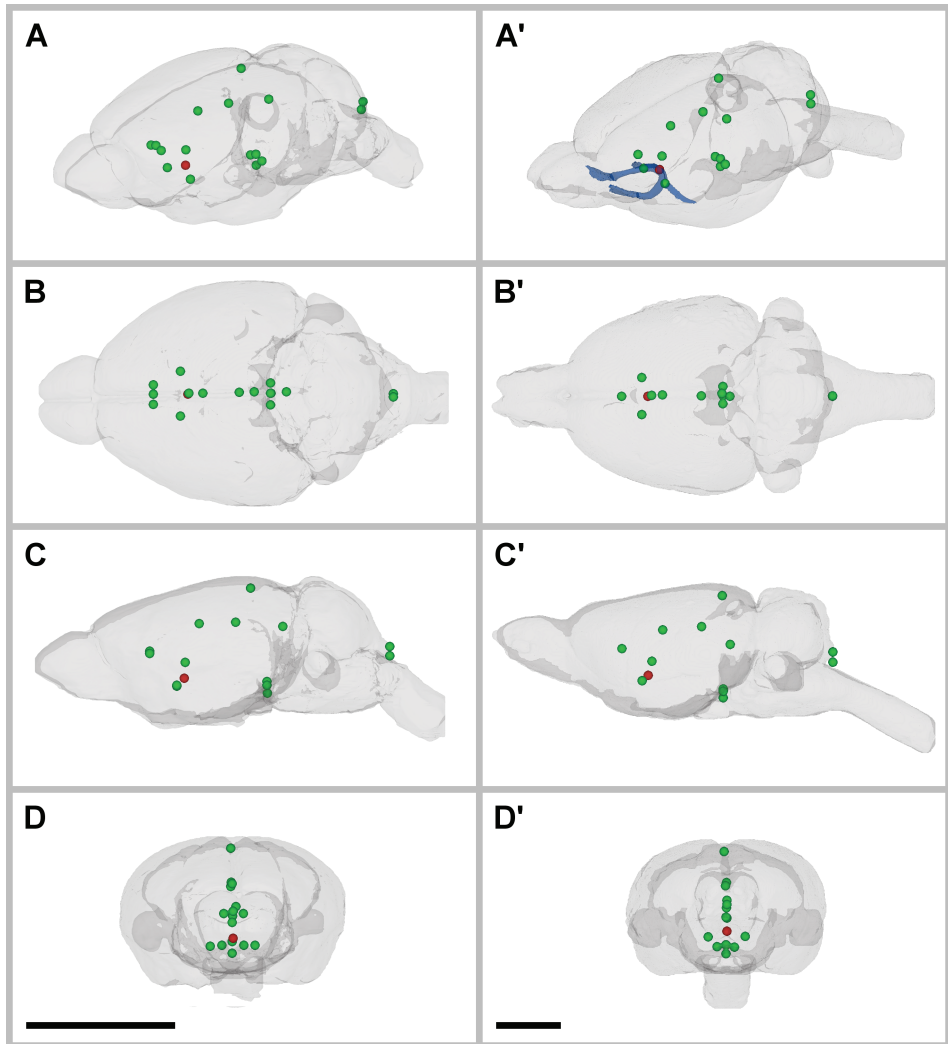


**Figure 5** | Spatial distribution of the anatomical landmark set in the Waxholm Space templates for the mouse (**A-D**) and rat brain (**A'-D'**). The position of 16 mouse and 14 rat brain landmarks (green dots) are illustrated in oblique (**A, A'**), top (**B, B'**), lateral (**C, C'**) and front (**D, D'**) view. The brain outline (gray shadow), the WHS origin (red dot), and the anterior commissure (blue structure in **A'**) are shown for reference. Scale bar: 5 mm

The main advantage of using a standard landmark set over an ad-hoc selection of landmarks lies in the consistently high spatial identification accuracy of standard landmarks. The performance of landmark-based registration can be described by the mean displacement error between landmark pairs after alignment. This error is proportional to  $1/\sqrt{N}$  where N represents the number of landmark points (Hill and Hawkes, 1994). Consequently, fewer landmarks are sufficient to reach the same level of alignment when those landmarks are identified with high accuracy (Zuk and Atkins, 1996). To specifically enhance alignment in regions of interest, further local landmarks may be used (West et al. 2001). The spatial distribution of the landmarks throughout the mouse and rat brain is illustrated in Figure 5. A relatively even coverage has been achieved in subcortical regions in both anteroposterior and dorsoventral direction. Since the mediolateral position of most landmarks is defined by the midsagittal plane or symmetrical anatomical features in its proximity, additional landmarks may be defined further laterally in the cerebral cortex and in the cerebellum to maximize local alignment in these brain regions.

Landmark-based registration provides a relatively simple, flexible and universal method for integration of diverse datasets in Waxholm Space. Since the alignment process does not involve similarity calculations on the voxel level, it is computationally less expensive compared to intensity-based methods. The transformation result can be used as a precursor to a more elaborate intensity-based alignment between images with a high level of anatomical detail and similar contrast properties. The availability of a shared set of standard landmarks across the mouse and rat brain offers the perspective of comparative analysis of anatomical images across strains and species. Recent developments in MRI-based atlas of the neonatal rat brain (Calabrese et al. 2013) also pose the question whether some of these landmarks can be identified through developmental stages, opening the possibility to improve the depth of the atlas by propagation of relevant WHS atlas delineations.

## ***Alignment of microscopic image series to MRI***

Volumetric registration methods based on anatomical landmarks or image intensity require the overall spatial integrity of the brain to be preserved or reconstructed. Microscopic image material, unless acquired from whole-brain 3D microscopy (Osten and Margrie, 2013) or subjected to lengthy reconstruction procedures (Zakiewicz et al. 2015), is not compatible with these methods. Alignment of comprehensive image series to traditional book atlases is limited by the viewing angle and the spacing of the atlas, and involves significant manual effort. Atlases based on isotropic MRI enable a different alignment approach via generation of oblique atlas plates that closely match the sectioning angle of the experimental series (for an overview of methods and examples, see Osechinskiy and Kruggel, 2011). While multiple relevant MRI viewer software are available (Table 2), section to volume alignment has until recently not been supported for large series of images.

We designed a workflow for section-based processing and alignment of image series that facilitates assignment of 3D anatomical location to data embedded in serial sections spanning the entire brain (Paper III). The alignment module of the workflow allows fast and accurate registration between large series of images and a selected volumetric atlas, e.g. the Waxholm Space atlases of the mouse and rat brain. A typical anchoring timeframe for four hundred sections, including manual adjustments to individual images and final validation, varies between a few hours and two working days depending on the overall quality of the section material, the stability of the sectioning angle throughout the series, the type and brightness of staining, and the level of experience in anatomy and in the use of the software. The amount of necessary manual interaction is minimized by iterative propagation of alignment parameters across not yet validated sections, repeated in real time after each finalized section anchoring. As a result of this strategy, manual steps are practically reduced to in-plane adjustments after the alignment of 5-10 key sections. The propagation algorithm also takes into account missing sections based on serial numbering, so that incomplete series can also be aligned.

**Table 2** | Viewer software for MRI-based atlases

<b>Software name</b>	<b>Slicing angle</b>	<b>2D overlay</b>	<b>Reference</b>
ITK-SNAP	standard	no	<a href="http://www.itksnap.org/">http://www.itksnap.org/</a>
NeuroTerrain	standard and oblique	no	Gustafson et al. 2007 (discontinued)
SHIVA	standard and oblique	no	<a href="http://www.loni.usc.edu/Software/moreinfo.php?package=SHIVA">http://www.loni.usc.edu/Software/moreinfo.php?package=SHIVA</a>
Caret	standard and oblique	no	<a href="http://brainvis.wustl.edu/wiki/index.php/Caret&gt;About">http://brainvis.wustl.edu/wiki/index.php/Caret&gt;About</a>
MNI Display	standard and oblique	no	<a href="http://www.bic.mni.mcgill.ca/software/Display/Display.html">http://www.bic.mni.mcgill.ca/software/Display/Display.html</a>
3D Slicer	standard and oblique	no	<a href="http://www.slicer.org">http://www.slicer.org</a>
HistoloZee	standard and oblique	yes	<a href="http://picsl.upenn.edu/software/histolozee/">http://picsl.upenn.edu/software/histolozee/</a>
AlignII	standard and oblique	yes	Paper III; <a href="https://www.nitrc.org/projects/cutnii">https://www.nitrc.org/projects/cutnii</a>

Our alignment procedure is built on the visual similarity of section images to structural MRI. This may have a limiting effect on anchoring accuracy for image series with less anatomical contrast, e.g. sections without counterstaining. In such cases, an alternative route may be the coarse co-registration of the series based on section outlines, followed by volumetric alignment to MRI and section-based manual adjustments (HistoloZee, see Table 2). Zooming functionality would further aid the interpretation of high resolution microscopic images. The current affine registration tools permit either global or local alignment, as individual regions in a section image cannot be aligned independently. For similar reasons, images of brain regions physically divided during sectioning, e.g. the cortical hemispheres, the cerebellum, or the inferior colliculus, cannot be aligned accurately at the same time. This could be overcome by splitting the images or by the implementation of non-linear alignment methods. Further development possibilities for the alignment module include the automation of coordinate acquisition for regions of interest in Waxholm Space, and integration with online data repositories such as the Rodent Brain Navigator (Moene et al. 2011; <http://rbwb.org>).

### ***Localization of labeling in brain-wide microscopy datasets***

The alignment of microscopic image series to a reference atlas is often motivated by the need to determine the anatomical situation of labeled elements, e.g. cells, fibers, proteins, or DNA, embedded in the images. We developed image processing modules that automate the detection of two types of axonal labeling in large series of section images, and offer basic tools for spatial analysis of the detected labeling. The resulting labeling maps record the location of labeling detected in the images and the size of the area occupied by labeled cells and axons. Compared to manual methods for quantification of labeling strength in whole-brain image material, such as manual point coding (Leergaard et al. 2000), or scoring according to a density rating system (Zakiewicz et al. 2014), our automatic detection method does not categorize labeling other than “detected” or “not detected”. Based on these binary maps, additional processing steps may be added to the workflow for measuring the density of labeling in selected regions, or labeling distribution over larger

regions or the whole brain. Since our image processing modules do not quantify stain intensity or relate it to labeling strength, concerns raised regarding the nonlinearity of the stain separation method Colour Deconvolution under polychromatic light conditions (Haub and Meckel, 2015), and the broad and unstable spectrum of DAB (diaminobenzidine; van der Loos, 2008) used as the chromogen for visualizing the BDA tracer, do not compromise the generation of the labeling maps.

From the aspect of connecting whole-brain microscopy datasets to Waxholm Space, the most important benefits of the image processing modules stem from the automated steps that enable efficient, reliable, and reproducible extraction of labeling data from large series of images. After completed alignment, the labeling maps for each section image can be directly combined with the custom-generated atlas plates from the alignment module to perform region-based or coordinate-based analyses for the whole brain. WHS coordinates acquired for each data point, if plotted in the original 3D space of the non-distorted anatomical MRI, allow unwarped 3D visualization of labeling patterns throughout the brain in the context of anatomical regions delineated in the WHS atlas. This approach enables 3D spatial analysis of labeling data from series that are incomplete, distorted, contain multiple alternating stains, or otherwise represent complex cases for 3D reconstruction. The level of spatial error in such analyses depends on the accuracy of the underlying section-based alignment, at this point implemented as a set of affine transformations. To improve the accuracy of coordinate acquisition, the alignment may be refined locally in labeled regions without a need to achieve a good overall fit for the whole section, as would be the case for 3D reconstruction of the entire histological dataset.

The integration of section-based data in Waxholm Space plays an important role in improving the level of detail in the atlas (Imad et al. 2017), and reanalyzing and sharing legacy data in a 3D anatomical framework. The workflow modules for image processing and alignment bridge the gap between whole-brain image series and volumetric atlases, and enable efficient 3D spatial analysis of the data embedded in the images.

## Impact and adoption by the community

MRI-based atlases provide morphologically correct anatomical reference for spatial integration of 2D and 3D datasets from a variety of image modalities. For an image-based reference space such as Waxholm Space to be applied in practice, both the structural image volumes and the associated anatomical delineations have to be made publicly available. Experimental data may thus be registered to the anatomical MRI, and analyzed based on the volumetric delineations. Examples exist for recently published reference atlases based on MRI and DTI that do not share the volumetric image material the atlas is built upon, but instead keep the traditional book format (Paxinos et al. 2015; Wisner et al. 2016). Since newly acquired tomographic image volumes cannot be directly aligned to these 2D atlases, it is difficult to use the anatomical delineations for spatial analysis and interpretation of 3D data from the brain. Upon these considerations, we provide open access to all of our newly developed atlasing resources.

We share the Sprague Dawley reference atlas, the anatomical landmark positions for the mouse and the rat brain, software for image processing and alignment, and related documentation through multiple channels and formats for different types of analysis (see also Methods). While the core datasets are available through the NITRC repository, other web-based services and software packages have also incorporated and re-shared our results. The Scalable Brain Atlas (<http://scalablebrainatlas.incf.org>; Bakker et al. 2015) offers a browser-friendly viewer for the atlas with functionality to visualize the standard landmark set in 3D. The 3D Brain Atlas Reconstructor ([www.3dbar.org](http://www.3dbar.org); Majka et al. 2013) provides a web-based service that creates 3D reconstructions from any delineated brain region or tract in the form of smooth surface meshes. The MRI/DTI template and the delineations have been incorporated into the fMRI program package AFNI (Analysis of Functional Neuroimages, National Institute of Mental Health, USA; <https://afni.nimh.nih.gov/>) for direct spatial analysis of fMRI data. Finally, we share hierarchical labels for use with the PMOD/PNEURO software ([www.pmod.com](http://www.pmod.com)) for volume of interest-based analysis of PET and other volumetric images.



Since the publication of Papers I-III, the main results of this work have been used for integration of different types of 2D and 3D datasets into a common space, and localization of signal in both functional and structural image volumes (Table 3). The three-dimensional nature of our atlas has made it possible to illustrate complex spatial relationships between brain regions (Moser et al. 2014), and perform measurements of distances within the brain (Böhme and van Rienen, 2016; Weltman et al. 2016). 3D surface models of the delineations have been applied to depict the anatomical location of electrodes (Hu et al. 2015; Xia et al. 2016) and injection sites (Sugar and Witter, 2016), and to visualize cutting planes (Gesnik et al. 2017; Zakiewicz et al. 2015). In addition, two studies have used the position of cranial landmarks identified in the MRI template (He et al. 2016; Ng et al. 2016). The high quality image material and the delineations published in Paper I have been used as a starting point for building a detailed atlas of the hippocampal region (Boccaro et al. 2015; Kjonigsen et al. 2015) and an *in vivo* atlas of the Wistar strain (Huang et al. 2016), with further developments on the way (Imad et al. 2017). We provide the atlas under a ShareAlike (CC-BY-NC-SA) license to ensure that future atlas versions remain open and freely available to the neuroscience community.

**Table 3** | Application of the new atlas resources in assignment of anatomical location to experimental data

<b>Application area</b>	<b>Image modality</b>	<b>2D / 3D</b>	<b>References</b>
Localization of signal detected by <i>in vivo</i> functional imaging	MEMRI	3D	Brunnquell et al. 2016
	BOLD fMRI	3D	Pawela et al. 2017
	PET	3D	Pottier et al. 2017
Interpretation and spatial analysis of structural images	FDG-PET	3D	Ladd et al. 2017; Thomas et al. 2016
	<i>ex vivo</i> and <i>in vivo</i> MRI	3D	Biezonski et al. 2016; Hsieh et al. 2017
	diffusion tensor imaging	3D	Kuo et al. 2017
Spatial integration of image series	microscopy (BF / FL)	2D	Dempsey et al. 2017; Olivares-Moreno et al. 2017
	autoradiography, PLI	2D	Schubert et al. 2016
Standard template for registration and spatial normalization	MRI	3D	Hsieh et al. 2016
	STPT	3D	Leergaard et al. 2014
	imaging mass spectrometry	3D	Verbeeck et al. 2017

- MEMRI** Manganese-enhanced MRI
- BF / FL** Brightfield / fluorescence
- BOLD** Blood-oxygen-level dependent
- FDG** Fluorodeoxyglucose
- PLI** Polarized light imaging
- STPT** Serial two-photon tomography

## CONCLUSIONS

The main contributions of this work include the first comprehensive MRI-based anatomical reference atlas of the Sprague Dawley rat brain, implementation of the Waxholm Space standard in this atlas, and development of methods and software for alignment and spatial analysis of whole-brain image data to this reference. Beyond the most immediate impact of our results related to anatomical localization of regions of interest in multimodality data, our work demonstrates how non-volumetric datasets such as microscopic image series, traditionally analyzed manually using stereotaxic atlases, can be efficiently connected to next-generation volumetric atlases through automated analytical workflows. In addition to compatibility with both 2D and 3D data on the image level, our atlas is interoperable with the stereotaxic space, and potentially with other atlas resources, on the level of standard spatial coordinates. Thus, alignment to the isotropic MRI facilitates querying of detailed anatomical information from stereotaxic atlases for spatial analysis of datasets where the acquisition angle would not allow direct comparison to a book atlas.

Volumetric maps of the rat brain are in high demand, as demonstrated by over 50 citations of Papers I-III, and close to 5000 downloads of our shared atlas files from the INCF Software Center and NITRC. We have been contacted by multiple researchers in search of more detailed delineations of individual regions, and new initiatives have been taken for the expansion of the atlas. The reference atlas, the anatomical landmarks, and the workflow module for section to volume alignment have also been utilized in relation to the rodent atlas efforts of the Human Brain Project ([www.humanbrainproject.eu/en/explore-the-brain](http://www.humanbrainproject.eu/en/explore-the-brain)), with the perspective of building a multi-level data enriched atlas of the rodent and ultimately of the human brain. We conclude that our work has contributed to advancing the field from coordinate-based to image-based reference atlases, and from a centralized approach to atlas development towards collaborative atlas.



## REFERENCES

- Alexander AL, Lee JE, Lazar M, and Field AS (2007) **Diffusion tensor imaging of the brain**. *Neurotherapeutics* 4, 316-329.  
DOI: 10.1016/j.nurt.2007.05.011
- Ali AA, Dale AM, Badea A, and Johnson GA (2005) **Automated segmentation of neuroanatomical structures in multispectral MR microscopy of the mouse brain**. *Neuroimage* 27, 425-435.  
DOI: 10.1016/j.neuroimage.2005.04.017
- Amunts K, Ebell C, Muller J, Telefont M, Knoll A, and Lippert T (2016) **The Human Brain Project: Creating a European Research Infrastructure to Decode the Human Brain**. *Neuron* 92, 574-581.  
DOI: 10.1016/j.neuron.2016.10.046
- Augustinack JC, Van Der Kouwe AJ, and Fischl B (2013) **Medial temporal cortices in ex vivo magnetic resonance imaging**. *J Comp Neurol* 521, 4177-4188. DOI: 10.1002/cne.23432
- Badea A, Ali-Sharief AA, and Johnson GA (2007) **Morphometric analysis of the C57BL/6J mouse brain**. *Neuroimage* 37, 683-693. DOI: 10.1016/j.neuroimage.2007.05.046
- Badea A, Johnson GA, and Williams RW (2009) **Genetic dissection of the mouse CNS using magnetic resonance microscopy**. *Curr Opin Neurol* 22, 379-386. DOI: 10.1097/WCO.0b013e32832d9b86
- Badea A and Johnson GA (2012) **Magnetic resonance microscopy**. *Anal Cell Pathol (Amst)* 35, 205-227. DOI: 10.3233/ACP-2011-0050
- Bakker R, Tiesinga P, and Kotter R (2015) **The Scalable Brain Atlas: Instant Web-Based Access to Public Brain Atlases and Related Content**. *Neuroinformatics* 13, 353-366. DOI: 10.1007/s12021-014-9258-x
- Baldock RA and Burger A (2012) **Biomedical atlases: systematics, informatics and analysis**. *Adv Exp Med Biol* 736, 655-677.  
DOI: 10.1007/978-1-4419-7210-1\_39
- Bello M, Ju T, Carson J, Warren J, Chiu W, and Kakadiaris IA (2007) **Learning-based segmentation framework for tissue images containing gene expression data**. *IEEE Trans Med Imaging* 26, 728-744.  
DOI: 10.1109/TMI.2007.895462

- Biezonski D, Shah R, Krivko A, Cha J, Guilfoyle DN, Hrabe J, Gerum S, Xie S, Duan Y, Bansal R, Leventhal BL, Peterson BS, Kellendonk C, and Posner J (2016) **Longitudinal magnetic resonance imaging reveals striatal hypertrophy in a rat model of long-term stimulant treatment.** *Transl Psychiatry* 6, e884. DOI: 10.1038/tp.2016.158
- Boccarda CN, Kjonigsen LJ, Hammer IM, Bjaalie JG, Leergaard TB, and Witter MP (2015) **A three-plane architectonic atlas of the rat hippocampal region.** *Hippocampus* 25, 838-857. DOI: 10.1002/hipo.22407
- Böhme A and van Rienen U (2016) **A comparative study of approaches to compute the field distribution of deep brain stimulation in the Hemiparkinson rat model.** *Conf Proc IEEE Eng Med Biol Soc* 2016, 5821-5824. DOI: 10.1109/EMBC.2016.7592051
- Brevik A, Leergaard TB, Svanevik M, and Bjaalie JG (2001) **Three-dimensional computerised atlas of the rat brain stem precerebellar system: approaches for mapping, visualization, and comparison of spatial distribution data.** *Anat Embryol (Berl)* 204, 319-332.
- Brun CC, Nicolson R, Lepore N, Chou YY, Vidal CN, Devito TJ, Drost DJ, Williamson PC, et al. (2009) **Mapping brain abnormalities in boys with autism.** *Hum Brain Mapp* 30, 3887-3900. DOI: 10.1002/hbm.20814
- Brunnquell CL, Hernandez R, Graves SA, Smit-Oistad I, Nickles RJ, Cai W, Meyerand ME, and Suzuki M (2016) **Uptake and retention of manganese contrast agents for PET and MRI in the rodent brain.** *Contrast Media Mol Imaging* 11, 371-380. DOI: 10.1002/cmml.1701
- Cabezas M, Oliver A, Llado X, Freixenet J, and Cuadra MB (2011) **A review of atlas-based segmentation for magnetic resonance brain images.** *Comput Methods Programs Biomed* 104, e158-177. DOI: 10.1016/j.cmpb.2011.07.015
- Calabrese E, Badea A, Watson C, and Johnson GA (2013) **A quantitative magnetic resonance histology atlas of postnatal rat brain development with regional estimates of growth and variability.** *Neuroimage* 71, 196-206. DOI: 10.1016/j.neuroimage.2013.01.017
- Chuang N, Mori S, Yamamoto A, Jiang H, Ye X, Xu X, Richards LJ, Nathans J, et al. (2011) **An MRI-based atlas and database of the developing mouse brain.** *Neuroimage* 54, 80-89. DOI: 10.1016/j.neuroimage.2010.07.043
- d'Arceuil H and de Crespigny A (2007) **The effects of brain tissue decomposition on diffusion tensor imaging and tractography.** *Neuroimage* 36, 64-68. DOI: 10.1016/j.neuroimage.2007.02.039

- Dempsey B, Le S, Turner A, Bokiniec P, Ramadas R, Bjaalie JG, Menuet C, Neve R, Allen AM, Goodchild AK, and McMullan S (2017) **Mapping and Analysis of the Connectome of Sympathetic Premotor Neurons in the Rostral Ventrolateral Medulla of the Rat Using a Volumetric Brain Atlas.** *Front Neural Circuits* 11, 9. DOI: 10.3389/fncir.2017.00009
- Dong H-W and the Allen Institute for Brain Science (2008) **Allen reference atlas: a digital color brain atlas of the C57Black/6J male mouse.** Wiley, Hoboken, NJ
- Evans AC, Janke AL, Collins DL, and Baillet S (2012) **Brain templates and atlases.** *Neuroimage* 62, 911-922. DOI: 10.1016/j.neuroimage.2012.01.024
- Flint JJ, Lee CH, Hansen B, Fey M, Schmidig D, Bui JD, King MA, Vestergaard-Poulsen P, et al. (2009) **Magnetic resonance microscopy of mammalian neurons.** *Neuroimage* 46, 1037-1040. DOI: 10.1016/j.neuroimage.2009.03.009
- Franklin KBJ and Paxinos G (1997) **The mouse brain in stereotaxic coordinates.** Academic Press, San Diego
- Franklin KBJ and Paxinos G (2008) **The mouse brain in stereotaxic coordinates.** Elsevier/Academic Press, Amsterdam, New York
- Gesnik M, Blaize K, Deffieux T, Gennisson JL, Sahel JA, Fink M, Picaud S, and Tanter M (2017) **3D functional ultrasound imaging of the cerebral visual system in rodents.** *Neuroimage* 149, 267-274. DOI: 10.1016/j.neuroimage.2017.01.071
- Grignon B, Mainard L, Delion M, Hodez C, and Oldrini G (2012) **Recent advances in medical imaging: anatomical and clinical applications.** *Surg Radiol Anat* 34, 675-686. DOI: 10.1007/s00276-012-0985-0
- Gustafson C, Bug WJ, and Nissanov J (2007) **NeuroTerrain – a client-server system for browsing 3D biomedical image data sets.** *BMC Bioinformatics* 8, 40. DOI: 10.1186/1471-2105-8-40
- Haub P and Meckel T (2015) **A Model based Survey of Colour Deconvolution in Diagnostic Brightfield Microscopy: Error Estimation and Spectral Consideration.** *Sci Rep* 5, 12096. DOI: 10.1038/srep12096
- Hawrylycz M, Baldock RA, Burger A, Hashikawa T, Johnson GA, Martone M, Ng L, Lau C, et al. (2011) **Digital atlasing and standardization in the mouse brain.** *PLoS Comput Biol* 7, e1001065. DOI: 10.1371/journal.pcbi.1001065

- He M, Liu Y, Shen J, Duan C, and Lu X (2016) **Upregulation of PLZF is Associated with Neuronal Injury in Lipopolysaccharide-Induced Neuroinflammation.** *Neurochem Res* 41, 3063-3073.  
DOI: 10.1007/s11064-016-2027-5
- Hill DLG and Hawkes DJ (1994) **Medical image registration using knowledge of adjacency of anatomical structures.** *Image and Vision Computing* 12, 173-178. DOI: 10.1016/0262-8856(94)90069-8
- Hillman EM (2007) **Optical brain imaging in vivo: techniques and applications from animal to man.** *J Biomed Opt* 12, 051402.  
DOI: 10.1117/1.2789693
- Hintiryan H, Gou L, Zingg B, Yamashita S, Lyden HM, Song MY, Grewal AK, Zhang X, et al. (2012) **Comprehensive connectivity of the mouse main olfactory bulb: analysis and online digital atlas.** *Front Neuroanat* 6, 30. DOI: 10.3389/fnana.2012.00030
- Hjornevik T, Leergaard TB, Darine D, Moldestad O, Dale AM, Willoch F, and Bjaalie JG (2007) **Three-dimensional atlas system for mouse and rat brain imaging data.** *Front Neuroinform* 1, 4.  
DOI: 10.3389/neuro.11.004.2007
- Hsieh MC, Tsai CY, Liao MC, Yang JL, Su CH, and Chen JH (2016) **Quantitative Susceptibility Mapping-Based Microscopy of Magnetic Resonance Venography (QSM-mMRV) for In Vivo Morphologically and Functionally Assessing Cerebromicrovasculature in Rat Stroke Model.** *PLoS One* 11, e0149602. DOI: 10.1371/journal.pone.0149602
- Hsieh MC, Kuo LW, Huang YA, and Chen JH (2017) **Investigating hyperoxic effects in the rat brain using quantitative susceptibility mapping based on MRI phase.** *Magn Reson Med* 77, 592-602.  
DOI: 10.1002/mrm.26139
- Hu L, Xia XL, Peng WW, Su WX, Luo F, Yuan H, Chen AT, Liang M, and Iannetti G (2015) **Was it a pain or a sound? Across-species variability in sensory sensitivity.** *Pain* 156, 2449-2457.  
DOI: 10.1097/j.pain.0000000000000316
- Huang S, Liu C, Dai G, Kim YR, and Rosen BR (2009) **Manipulation of tissue contrast using contrast agents for enhanced MR microscopy in ex vivo mouse brain.** *Neuroimage* 46, 589-599.  
DOI: 10.1016/j.neuroimage.2009.02.027



- Huang S, Lu Z, Huang W, Seramani S, Ramasamy B, Sekar S, Guan C, and Bhakoo K (2016) **"High-resolution in vivo Wistar rodent brain atlas based on T1 weighted image"**, 978825-978825-978826.
- Hurley RA and Taber KH (2008) **Imaging of eating disorders: multiple techniques to demonstrate the dynamic brain.** *J Neuropsychiatry Clin Neurosci* 20, iv-260. DOI: 10.1176/appi.neuropsych.20.3.iv
- Imad J, Wennberg AE, Osen KK, Clascá F, Csucs G, Coello C, Bjaalie JG, and Leergaard TB (2017) **"Expanding the Waxholm Space rat brain reference atlas using a data enriched magnetic resonance imaging template: new delineations of the auditory system, thalamus, and more"**. *Annual Meeting of the Society for Neuroscience*, Washington
- Johnson GA, Badea A, Brandenburg J, Cofer G, Fubara B, Liu S, and Nissanov J (2010) **Waxholm space: an image-based reference for coordinating mouse brain research.** *Neuroimage* 53, 365-372. DOI: 10.1016/j.neuroimage.2010.06.067
- Johnson GA, Calabrese E, Badea A, Paxinos G, and Watson C (2012) **A multidimensional magnetic resonance histology atlas of the Wistar rat brain.** *Neuroimage* 62, 1848-1856. DOI: 10.1016/j.neuroimage.2012.05.041
- Khazipov R, Zaynutdinova D, Ogievetsky E, Valeeva G, Mitrukhhina O, Manent JB, and Represa A (2015) **Atlas of the Postnatal Rat Brain in Stereotaxic Coordinates.** *Front Neuroanat* 9, 161. DOI: 10.3389/fnana.2015.00161
- Kjonigsen LJ, Leergaard TB, Witter MP, and Bjaalie JG (2011) **Digital atlas of anatomical subdivisions and boundaries of the rat hippocampal region.** *Front Neuroinform* 5, 2. DOI: 10.3389/fninf.2011.00002
- Kjonigsen LJ, Lillehaug S, Bjaalie JG, Witter MP, and Leergaard TB (2015) **Waxholm Space atlas of the rat brain hippocampal region: three-dimensional delineations based on magnetic resonance and diffusion tensor imaging.** *Neuroimage* 108, 441-449. DOI: 10.1016/j.neuroimage.2014.12.080
- Knickmeyer RC, Gouttard S, Kang C, Evans D, Wilber K, Smith JK, Hamer RM, Lin W, et al. (2008) **A structural MRI study of human brain development from birth to 2 years.** *J Neurosci* 28, 12176-12182. DOI: 10.1523/JNEUROSCI.3479-08.2008
- Kopec CD, Bowers AC, Pai S, and Brody CD (2011) **Semi-automated atlas-based analysis of brain histological sections.** *J Neurosci Methods* 196, 12-19. DOI: 10.1016/j.jneumeth.2010.12.007

- Kötter R and Wanke E (2005) **Mapping brains without coordinates.** *Philos Trans R Soc Lond B Biol Sci* 360, 751-766. DOI: 10.1098/rstb.2005.1625
- Kuo DP, Lu CF, Liou M, Chen YC, Chung HW, and Chen CY (2017) **Differentiation of the Infarct Core from Ischemic Penumbra within the First 4.5 Hours, Using Diffusion Tensor Imaging-Derived Metrics: A Rat Model.** *Korean J Radiol* 18, 269-278. DOI: 10.3348/kjr.2017.18.2.269
- Ladd AC, Brohawn DG, Thomas RR, Keeney PM, Berr SS, Khan SM, Portell FR, Shakenov MZ, Antkowiak PF, Kundu B, Tustison N, and Bennett JP (2017) **RNA-seq analyses reveal that cervical spinal cords and anterior motor neurons from amyotrophic lateral sclerosis subjects show reduced expression of mitochondrial DNA-encoded respiratory genes, and rhTFAM may correct this respiratory deficiency.** *Brain Research* 1667, 74-83. DOI: <https://doi.org/10.1016/j.brainres.2017.05.010>
- Leergaard TB, Lyngstad KA, Thompson JH, Taeymans S, Vos BP, De Schutter E, Bower JM, and Bjaalie JG (2000) **Rat somatosensory cerebropontocerebellar pathways: spatial relationships of the somatotopic map of the primary somatosensory cortex are preserved in a three-dimensional clustered pontine map.** *J Comp Neurol* 422, 246-266.
- Leergaard TB, Bjaalie JG, Devor A, Wald LL, and Dale AM (2003) **In vivo tracing of major rat brain pathways using manganese-enhanced magnetic resonance imaging and three-dimensional digital atlasing.** *Neuroimage* 20, 1591-1600.
- Leergaard TB, Coello C, Papp EA, Ragan T, and Bjaalie JG (2014) **"Registration of serial two-photon data to rodent brain Waxholm Space"** *Neuroinformatics 2014*, Leiden, Netherlands. Frontiers in Neuroinformatics, DOI: 10.3389/conf.fninf.2014.18.00059
- Lein ES, Hawrylycz MJ, Ao N, Ayres M, Bensinger A, Bernard A, Boe AF, Boguski MS, et al. (2007) **Genome-wide atlas of gene expression in the adult mouse brain.** *Nature* 445, 168-176. DOI: 10.1038/nature05453
- Lu H, Scholl CA, Zuo Y, Demny S, Rea W, Stein EA, and Yang Y (2010) **Registering and analyzing rat fMRI data in the stereotaxic framework by exploiting intrinsic anatomical features.** *Magn Reson Imaging* 28, 146-152. DOI: 10.1016/j.mri.2009.05.019

- Ma Y, Hof PR, Grant SC, Blackband SJ, Bennett R, Slatest L, Mcguigan MD, and Benveniste H (2005) **A three-dimensional digital atlas database of the adult C57BL/6J mouse brain by magnetic resonance microscopy.** *Neuroscience* 135, 1203-1215.  
DOI: 10.1016/j.neuroscience.2005.07.014
- Ma Y, Smith D, Hof PR, Foerster B, Hamilton S, Blackband SJ, Yu M, and Benveniste H (2008) **In Vivo 3D Digital Atlas Database of the Adult C57BL/6J Mouse Brain by Magnetic Resonance Microscopy.** *Front Neuroanat* 2, 1. DOI: 10.3389/neuro.05.001.2008
- Majka P, Kublik E, Furga G, and Wojcik DK (2012) **Common atlas format and 3D brain atlas reconstructor: infrastructure for constructing 3D brain atlases.** *Neuroinformatics* 10, 181-197.  
DOI: 10.1007/s12021-011-9138-6
- Majka P, Kowalski JM, Chlodzinska N, and Wojcik DK (2013) **3D brain atlas reconstructor service – online repository of three-dimensional models of brain structures.** *Neuroinformatics* 11, 507-518.  
DOI: 10.1007/s12021-013-9199-9
- Moene I, Darine D, Ramachandran M, Leergaard TB, Bjaalie JG (2011) **"Rodent Brain Navigator: database and atlas system for microscopy and imaging data".** *4th INCF Congress of Neuroinformatics*, Boston, MA
- Moser EI, Roudi Y, Witter MP, Kentros C, Bonhoeffer T, and Moser MB (2014) **Grid cells and cortical representation.** *Nat Rev Neurosci* 15, 466-481.  
DOI: 10.1038/nrn3766
- Ng KF, Anderson S, Mayo P, Aung HH, Walton JH, and Rutledge JC (2016) **Characterizing blood-brain barrier perturbations after exposure to human triglyceride-rich lipoprotein lipolysis products using MRI in a rat model.** *Magn Reson Med* 76, 1246-1251.  
DOI: 10.1002/mrm.25985
- Nie B, Chen K, Zhao S, Liu J, Gu X, Yao Q, Hui J, Zhang Z, et al. (2013) **A rat brain MRI template with digital stereotaxic atlas of fine anatomical delineations in paxinos space and its automated application in voxel-wise analysis.** *Hum Brain Mapp* 34, 1306-1318.  
DOI: 10.1002/hbm.21511
- Niedworok CJ, Brown AP, Jorge Cardoso M, Osten P, Ourselin S, Modat M, and Margrie TW (2016) **aMAP is a validated pipeline for registration and segmentation of high-resolution mouse brain data.** *Nat Commun* 7, 11879. DOI: 10.1038/ncomms11879

- Oguz I, Yaxley R, Budin F, Hoogstoel M, Lee J, Maltbie E, Liu W, and Crews FT (2013) **Comparison of magnetic resonance imaging in live vs. post mortem rat brains.** *PLoS One* 8, e71027. DOI: 10.1371/journal.pone.0071027
- Oh SW, Harris JA, Ng L, Winslow B, Cain N, Mihalas S, Wang Q, Lau C, et al. (2014) **A mesoscale connectome of the mouse brain.** *Nature* 508, 207-214. DOI: 10.1038/nature13186
- Okamura-Oho Y, Shimokawa K, Takemoto S, Hirakiyama A, Nakamura S, Tsujimura Y, Nishimura M, Kasukawa T, et al. (2012) **Transcriptome tomography for brain analysis in the web-accessible anatomical space.** *PLoS One* 7, e45373. DOI: 10.1371/journal.pone.0045373
- Olivares-Moreno R, Moreno-Lopez Y, Concha L, Martinez-Lorenzana G, Condes-Lara M, Cordero-Erausquin M, and Rojas-Piloni G (2017) **The rat corticospinal system is functionally and anatomically segregated.** *Brain Struct Funct.* DOI: 10.1007/s00429-017-1447-6
- Osechinskiy S and Kruggel F (2011) **Slice-to-Volume Nonrigid Registration of Histological Sections to MR Images of the Human Brain.** *Anat Res Int* 2011, 287860. DOI: 10.1155/2011/287860
- Osen KK, Wennberg AE, Oliveira AL, Manurung L, Zoabi M, Papp EA, Leergaard, TB (in preparation) **Waxholm Space atlas of the rat brain auditory system: Three-dimensional delineations based on magnetic resonance and diffusion tensor imaging**
- Osten P and Margrie TW (2013) **Mapping brain circuitry with a light microscope.** *Nat Methods* 10, 515-523. DOI: 10.1038/nmeth.2477
- Otte A and Halsband U (2006) **Brain imaging tools in neurosciences.** *J Physiol Paris* 99, 281-292. DOI: 10.1016/j.jphysparis.2006.03.011
- Pawela CP, Kramer JM, and Hogan QH (2017) **Dorsal root ganglion stimulation attenuates the BOLD signal response to noxious sensory input in specific brain regions: Insights into a possible mechanism for analgesia.** *Neuroimage* 147, 10-18. DOI: 10.1016/j.neuroimage.2016.11.046
- Paxinos G and Watson C (1982) **The rat brain in stereotaxic coordinates.** Academic Press, Sydney, New York
- Paxinos G, Watson C, Pennisi M, and Topple A (1985) **Bregma, lambda and the interaural midpoint in stereotaxic surgery with rats of different sex, strain and weight.** *J Neurosci Methods* 13, 139-143.

- Paxinos G and Watson C (2007) **The rat brain in stereotaxic coordinates**. Elsevier, Amsterdam, Boston
- Paxinos G, Watson C, Calabrese E, Badea A, and Johnson GA (2015) **MRI/DTI Atlas of the Rat Brain**. Academic Press, San Diego
- Pottier G, Gomez-Vallejo V, Padro D, Boisgard R, Dolle F, Llop J, Winkeler A, and Martin A (2017) **PET imaging of cannabinoid type 2 receptors with [11C]A-836339 did not evidence changes following neuroinflammation in rats**. *J Cereb Blood Flow Metab* 37, 1163-1178. DOI: 10.1177/0271678X16685105
- Ruifrok AC and Johnston DA (2001) **Quantification of histochemical staining by color deconvolution**. *Anal Quant Cytol Histol* 23, 291-299.
- Rumple A, McMurray M, Johns J, Lauder J, Makam P, Radcliffe M, and Oguz I (2013) **3-dimensional diffusion tensor imaging (DTI) atlas of the rat brain**. *PLoS One* 8, e67334. DOI: 10.1371/journal.pone.0067334
- Schubert N, Axer M, Schober M, Huynh AM, Huysegoms M, Palomero-Gallagher N, Bjaalie JG, Leergaard TB, Kirlangic ME, Amunts K, and Zilles K (2016) **3D Reconstructed Cyto-, Muscarinic M2 Receptor, and Fiber Architecture of the Rat Brain Registered to the Waxholm Space Atlas**. *Front Neuroanat* 10, 51. DOI: 10.3389/fnana.2016.00051
- Schwarz AJ, Danckaert A, Reese T, Gozzi A, Paxinos G, Watson C, Merlo-Pich EV, and Bifone A (2006) **A stereotaxic MRI template set for the rat brain with tissue class distribution maps and co-registered anatomical atlas: application to pharmacological MRI**. *Neuroimage* 32, 538-550. DOI: 10.1016/j.neuroimage.2006.04.214
- Schweinhardt P, Fransson P, Olson L, Spenger C, and Andersson JL (2003) **A template for spatial normalisation of MR images of the rat brain**. *J Neurosci Methods* 129, 105-113.
- Shcherbatyy V, Carson J, Yaylaoglu M, Jackle K, Grabbe F, Brockmeyer M, Yavuz H, and Eichele G (2015) **A digital atlas of ion channel expression patterns in the two-week-old rat brain**. *Neuroinformatics* 13, 111-125. DOI: 10.1007/s12021-014-9247-0
- Stansberg C, Ersland KM, Van Der Valk P, and Steen VM (2011) **Gene expression in the rat brain: high similarity but unique differences between frontomedial-, temporal- and occipital cortex**. *BMC Neurosci* 12, 15. DOI: 10.1186/1471-2202-12-15
- Sugar J and Witter MP (2016) **Postnatal development of retrosplenial projections to the parahippocampal region of the rat**. *Elife* 5. DOI: 10.7554/eLife.13925

- Sun SW, Neil JJ, and Song SK (2003) **Relative indices of water diffusion anisotropy are equivalent in live and formalin-fixed mouse brains.** *Magn Reson Med* 50, 743-748. DOI: 10.1002/mrm.10605
- Swanson LW (2004) **Brain maps III: structure of the rat brain.** Academic Press, Oxford
- Talairach J, Szikla G, Tournoux P, Prosalentis A, Bordas-Ferrier M, Covello L, Jacob M, and Mempel E (1967) **Atlas d'Anatomie Stéréotaxique du Télencéphale: Etudes Anatomico-Radiologiques.** Masson et Cie, Paris
- Talairach J and Tournoux P (1988) **Co-planar Stereotaxic Atlas of the Human Brain: 3-Dimensional Proportional System – an Approach to Cerebral Imaging.** Thieme Medical Publishers, New York
- Thomas RR, Keeney PM, Berr SB, Khan SM, Portell FR, Shakenov MZ, Antkowiak PF, Kundu B, Tustison N, Brohawn DG; Bennett JP (2016) **Recombinant Human TFAM Stimulates Rat Brain, Rat Cervical Spinal Cord and Human Neural Stem Cell Mitochondrial Bioenergetics.** (manuscript) Neurodegeneration Therapeutics, Inc.  
URL: [http://ndtherapeutics.org/wp-content/uploads/2016/05/rev3\\_Mitochondrion\\_Weekly-Intravenous-Treatment-with-rhTFAM\\_1-16-16.pdf](http://ndtherapeutics.org/wp-content/uploads/2016/05/rev3_Mitochondrion_Weekly-Intravenous-Treatment-with-rhTFAM_1-16-16.pdf)
- Toga AW (2002) **Imaging databases and neuroscience.** *Neuroscientist* 8, 423-436.
- Ungerstedt U (1971) **Stereotaxic mapping of the monoamine pathways in the rat brain.** *Acta Physiol Scand Suppl* 367, 1-48.
- Valdes-Hernandez PA, Sumiyoshi A, Nonaka H, Haga R, Aubert-Vasquez E, Ogawa T, Iturria-Medina Y, Riera JJ, et al. (2011) **An in vivo MRI Template Set for Morphometry, Tissue Segmentation, and fMRI Localization in Rats.** *Front Neuroinform* 5, 26. DOI: 10.3389/fninf.2011.00026
- Van Der Loos CM (2008) **Multiple immunoenzyme staining: methods and visualizations for the observation with spectral imaging.** *J Histochem Cytochem* 56, 313-328. DOI: 10.1369/jhc.2007.950170
- Van Essen DC (2002) **Windows on the brain: the emerging role of atlases and databases in neuroscience.** *Curr Opin Neurobiol* 12, 574-579.
- Venneti S, Lopresti BJ, and Wiley CA (2013) **Molecular imaging of microglia/macrophages in the brain.** *Glia* 61, 10-23.  
DOI: 10.1002/glia.22357

- Veraart J, Leergaard TB, Antonsen BT, Van Hecke W, Blockx I, Jeurissen B, Jiang Y, Van Der Linden A, et al. (2011) **Population-averaged diffusion tensor imaging atlas of the Sprague Dawley rat brain.** *Neuroimage* 58, 975-983. DOI: 10.1016/j.neuroimage.2011.06.063
- Verbeeck N, Spraggins JM, Murphy MJM, Wang HD, Deutch AY, Caprioli RM, and Van De Plas R (2017) **Connecting imaging mass spectrometry and magnetic resonance imaging-based anatomical atlases for automated anatomical interpretation and differential analysis.** *Biochim Biophys Acta* 1865, 967-977. DOI: 10.1016/j.bbapap.2017.02.016
- Weltman A, Yoo J, and Meng E (2016) **Flexible, Penetrating Brain Probes Enabled by Advances in Polymer Microfabrication.** *Micromachines* 7, 180.
- West JB, Fitzpatrick JM, Toms SA, Maurer CR Jr., and Maciunas RJ (2001) **Fiducial point placement and the accuracy of point-based, rigid body registration.** *Neurosurgery* 48, 810-816; discussion 816-817.
- Wisner K, Odintsov B, Brozoski D, and Brozoski TJ (2016) **Ratat1: A Digital Rat Brain Stereotaxic Atlas Derived from High-Resolution MRI Images Scanned in Three Dimensions.** *Front Syst Neurosci* 10, 64. DOI: 10.3389/fnsys.2016.00064
- Xia XL, Peng WW, Iannetti GD, and Hu L (2016) **Laser-evoked cortical responses in freely-moving rats reflect the activation of C-fibre afferent pathways.** *Neuroimage* 128, 209-217. DOI: 10.1016/j.neuroimage.2015.12.042
- Yu Y, Fuscoe JC, Zhao C, Guo C, Jia M, Qing T, Bannon DI, Lancashire L, et al. (2014) **A rat RNA-Seq transcriptomic BodyMap across 11 organs and 4 developmental stages.** *Nat Commun* 5, 3230. DOI: 10.1038/ncomms4230
- Zakiewicz IM, Van Dongen YC, Leergaard TB, and Bjaalie JG (2011) **Workflow and atlas system for brain-wide mapping of axonal connectivity in rat.** *PLoS One* 6, e22669. DOI: 10.1371/journal.pone.0022669
- Zakiewicz IM, Bjaalie JG, and Leergaard TB (2014) **Brain-wide map of efferent projections from rat barrel cortex.** *Front Neuroinform* 8, 5. DOI: 10.3389/fninf.2014.00005
- Zakiewicz IM, Majka P, Wojcik DK, Bjaalie JG, and Leergaard TB (2015) **Three-Dimensional Histology Volume Reconstruction of Axonal Tract Tracing Data: Exploring Topographical Organization in Subcortical Projections from Rat Barrel Cortex.** *PLoS One* 10, e0137571. DOI: 10.1371/journal.pone.0137571

- Zaslavsky I, Baldock RA, and Boline J (2014) **Cyberinfrastructure for the digital brain: spatial standards for integrating rodent brain atlases.** *Front Neuroinform* 8, 74. DOI: 10.3389/fninf.2014.00074
- Zilles K (2012) **The Cortex of the Rat: A Stereotaxic Atlas.** Springer Science & Business Media, Berlin
- Zuk TD and Atkins MS (1996) **A comparison of manual and automatic methods for registering scans of the head.** *IEEE Trans Med Imaging* 15, 732-744. DOI: 10.1109/42.538950

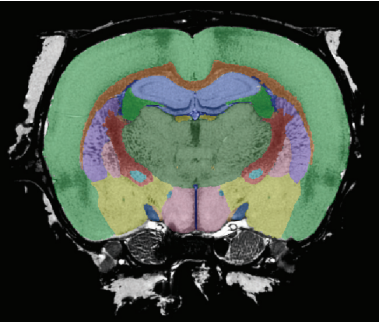
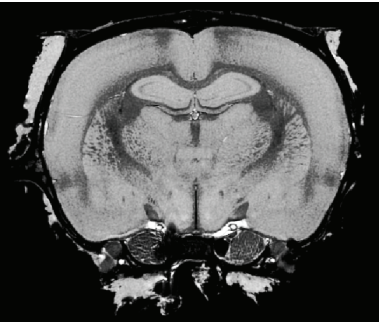
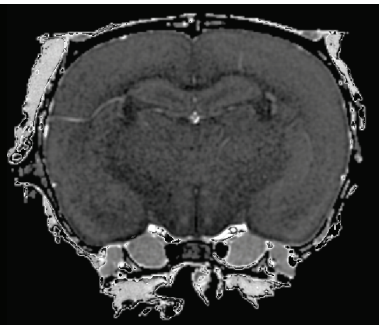


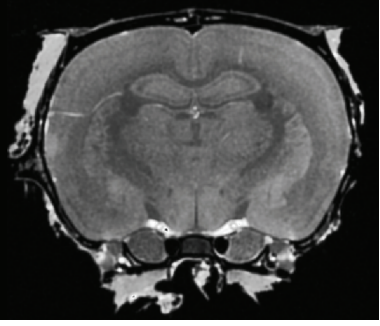
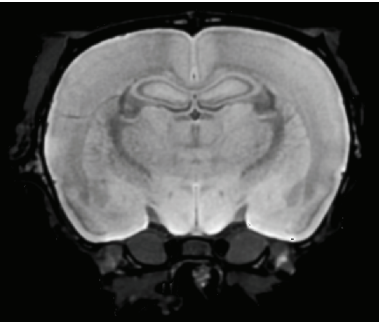
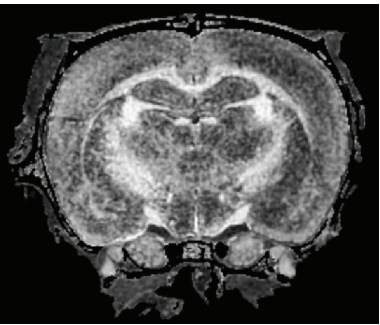
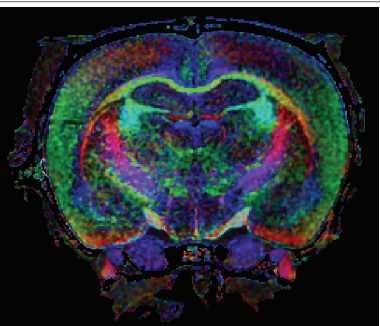
# APPENDIX



# Waxholm Space atlas of the Sprague Dawley rat brain

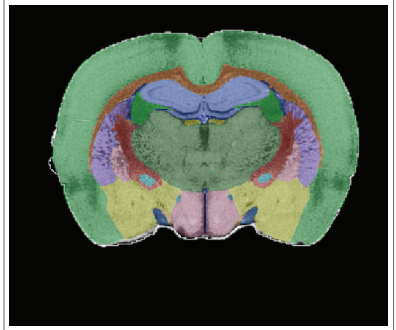
List and description of shared atlas and template files

File name	Description	Preview
<b>Volumetric atlas (1024x512x512 voxels)</b>		
WHS_SD_rat_atlas_v1.nii.gz	Volumetric atlas of 76 anatomical structures	
WHS_SD_rat_atlas_v1.label	Label file for ITK-SnAP (.label)	
MBAT_WHS_SD_rat_atlas_v1.zip	MBAT-ready atlas with label (.ilf) and startup file (.atlas)	
<b>MRI/DTI template</b>		
WHS_SD_rat_T2star.nii.gz	Anatomical MRI, $T_2^*$ -weighted gradient echo image at 39 $\mu\text{m}$ original resolution (1024x512x512 voxels)	
WHS_SD_rat_ADC.nii.gz	Apparent Diffusion Coefficient (ADC) map resampled to 39 $\mu\text{m}$ resolution (1024x512x512 voxels). Also known as the "mean diffusivity" or "trace ADC" or "mean ADC"	

<p>WHS_SD_rat_b0.nii.gz</p>	<p>The DTI b0 image resampled to 39 <math>\mu\text{m}</math> resolution (1024x512x512 voxels). A <math>T_2</math>-weighted image acquired without any diffusion sensitizing gradients</p>	
<p>WHS_SD_rat_DWI.nii.gz</p>	<p>Diffusion weighted image map resampled to 39 <math>\mu\text{m}</math> resolution (1024x512x512 voxels). Mean diffusion weighted image, also referred to as the isotropic diffusion image</p>	
<p>WHS_SD_rat_FA.nii.gz</p>	<p>Fractional Anisotropy (FA) map resampled to 39 <math>\mu\text{m}</math> resolution (1024x512x512 voxels)</p>	
<p>WHS_SD_rat_FA_color.nii.gz</p>	<p>Color FA map resampled to 39 <math>\mu\text{m}</math> resolution (1024x512x512 voxels).  Combines the FA and primary eigen vector to 24-bit color RGB where intensity is given by relative FA value and color is assigned to directions (RGB to xyz respectively)</p>	
<p>WHS_SD_rat_DTI_512.zip</p>	<p>All DTI volumes at original 78 <math>\mu\text{m}</math> resolution (512x512x256 voxels)</p>	

WHS\_SD\_rat\_brainmask.nii.gz

A volumetric mask to hide non-brain image elements, resampled to 39  $\mu\text{m}$  resolution (1024x512x512 voxels)





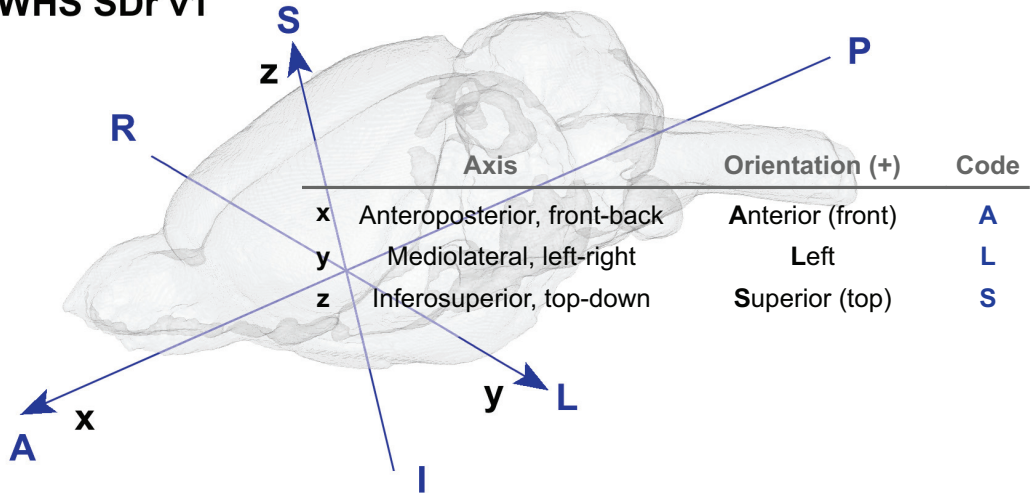
# Waxholm Space atlas of the Sprague Dawley rat brain

## Coordinate system orientation v1 vs v1.01

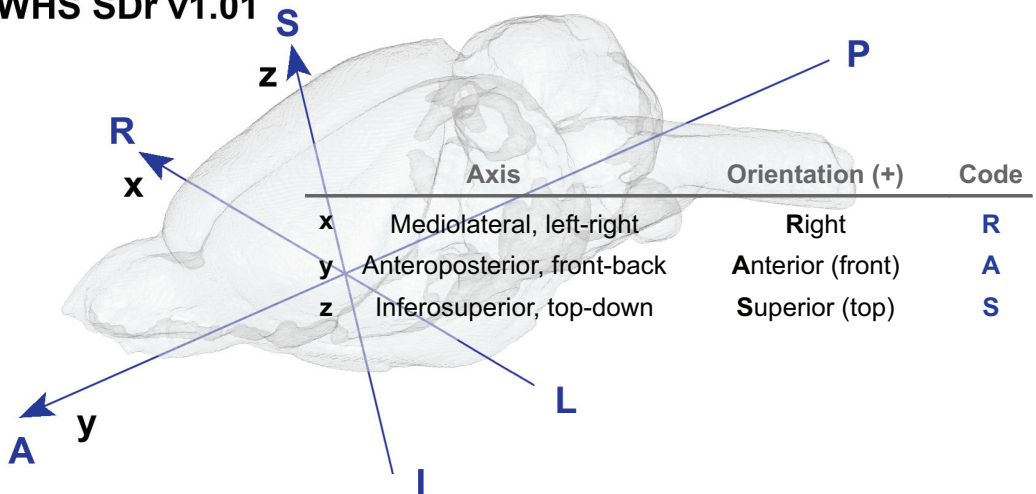
Neural Systems Laboratory, E. A. Papp and J. G. Bjaalie

16 July 2014

### WHS SDr v1



### WHS SDr v1.01



# Waxholm Space atlas of the Sprague Dawley rat brain

## Coordinates v1 vs v1.01

Neural Systems Laboratory, E. A. Papp and J. G. Bjaalie

16 July 2014

WHS SDr v1		WHS SDr v1.01					
		High resolution (39 $\mu$ m)			Low resolution (78 $\mu$ m)		
Voxels	WHS voxels	Voxels	WHS voxels	WHS mm	Voxels	WHS voxels	WHS mm

### WHS origin

x	623	0	244	0	0.0000000	122	0	0.0000000
y	268	0	623	0	0.0000000	311.5 <sup>1</sup>	0	0.0000000
z	248	0	248	0	0.0000000	124	0	0.0000000

### Bregma

x	653	30	246	2	0.0781250	123	1	0.0781250
y	266	-2	653	30	1.1718750	326.5 <sup>1</sup>	15	1.1718750
z	440	192	440	192	7.5000000	220	96	7.5000000

### Lambda

x	442	-181	244	0	0.0000000	122	0	0.0000000
y	268	0	442	-181	-7.0703125	221	-90.5 <sup>1</sup>	-7.0703125
z	464	216	464	216	8.4375000	232	108	8.4375000

### Calculating v1.01 coordinates for any point with v1 coordinates (a; b; c)

x	a	a - 623	512 - b	$\frac{(512-b) - 244}{[(512-b) - 244]}$	$0.0390625^* \frac{(512-b) - 244}{[(512-b) - 244]}$	$\frac{(512-b)}{2}$	$\frac{(512-b)}{2} - 122$	$0.078125^* \frac{(512-b)}{2} - 122]$
y	b	b - 268	a	a - 623	$0.0390625^* (a - 623)$	a/2	a/2-311.5	$0.078125^* (a/2-311.5)$
z	c	c - 248	c	c - 248	$0.0390625^* (c - 248)$	c/2	c/2-124	$0.078125^* (c/2-124)$

<sup>1</sup> We use voxel coordinates with a .5 value so that identical metric WHS coordinates are retrieved for identical anatomical points of interest in both the high resolution and the low resolution datasets. This is realized in the NIfTI files by storing the WHS origin in metric coordinates (see the `qoffset` and `srow` fields of the header).

Note that voxel coordinates are not identical to slice numbers. For example, in an 512\*512\*1024 volume, slice numbers range between (1..512; 1..512; 1..1024), while voxel coordinates range between (0..511; 0..511; 0..1023).



# Waxholm Space atlas of the Sprague Dawley rat brain

## Release notes v1.01

Neural Systems Laboratory, E. A. Papp and J. G. Bjaalie

16 July 2014

---

## TOC

[Why a new release?](#)

[What's new?](#)

[What's unchanged?](#)

[How to migrate from the previous version?](#)

[Will the original data still be available?](#)

[Is this a stable version? Is this the final version?](#)

---

## Why a new release?

The main goal of the v1.01 release is to standardize the orientation of the volumetric datasets according to [NIfTI-1 format](#) defaults, and to set the Waxholm Space origin so that coordinates can be read off directly using publicly available software, with a focus on [ITK-SNAP](#) and [MBAT](#).

[\[back to top\]](#)

---

## What's new?

- All high resolution (39 $\mu$ m) and low resolution (78 $\mu$ m) datasets, originally in ALS orientation, are transformed to standard RAS orientation.
- As a result, the order and the orientation of the x and y axes have changed, and the WHS origin has new voxel coordinates.
- The WHS origin is now set as the origin of the NIfTI coordinate system in all files.
- Voxel dimensions are included in full precision in the NIfTI header for all images.
- Documentation is added for comparing coordinate system orientation between v1 and v1.01; describing coordinates for the WHS origin, bregma, and lambda; and for calculating coordinates from v1 to v1.01.
- DTI color coding is now standard in both high resolution (39 $\mu$ m) and low resolution (78 $\mu$ m) color FA maps: Red = left-right (LR), Green = anteroposterior (AP), Blue = inferosuperior (IS).

[\[back to top\]](#)

---

## What's unchanged?

The anatomical boundaries in the segmentation, and the corresponding label files (.label, .ilf) are identical to those in version 1. The NIfTI atlas volume is reoriented the same way as the MRI/DTI template. Anatomical MRI and DTI image content is unchanged apart from swapped DTI color channels.

[\[back to top\]](#)

---

## How to migrate from the previous version?

WHS coordinates acquired in version 1 are easily transformed to v1.01 coordinates, see **Coordinates v1 vs 1.01** table for calculating new coordinates. Segmentations created on top of ALS-oriented v1 volumes need to be reoriented to RAS to match the v1.01 volumes.

[\[back to top\]](#)

---

## Will the original data still be available?

Yes, the original datasets will stay available for reference. Nevertheless we suggest using version 1.01 since this is in standard orientation with the WHS origin set, making it easier to navigate Waxholm Space.

[\[back to top\]](#)

---

## Is this a stable version? Is this the final version?

Version 1.01 is stable in the sense that technical issues concerning non-standard volumes are resolved. It is not the final version as segmentations will be evolving.

[\[back to top\]](#)

---

## Acknowledgments

We would like to thank Gergely Csúcs for expert technical assistance with standardization of the NIfTI volumes. Thanks to Rembrandt Bakker and Trygve B. Leergaard for valuable comments and advice.

# Waxholm Space atlas of the Sprague Dawley rat brain

## Release notes v2

Neural Systems Laboratory, T. B. Leergaard and J. G. Bjaalie

2 February 2015

---

## TOC

[What's new?](#)

[How to use the new atlas?](#)

[References](#)

---

## What's new?

Version 2 of the Waxholm Space atlas of the Sprague Dawley rat brain contains new and updated delineations of the hippocampal formation and parahippocampal region, as described in Kjonigsen et al. 2015. The new atlas includes 79 anatomical structures. 13 of these are new or revised delineations of the hippocampal formation and parahippocampal region. 66 structures are identical to those in v1.01, as described in Papp et al. 2014. Two structures (“neocortex” and “corpus callosum and associated subcortical white matter”) were adjusted to match the updated outer boundaries of the hippocampal formation and parahippocampal region.

[\[back to top\]](#)

---

## How to use the new atlas?

The atlas consists of volumetric delineations (.nii.gz) and corresponding labels containing the names of anatomical structures (.label). The atlas should be used together with the latest version of the MRI/DTI template (v1.01). A bundled zip download package of the typically used atlas and template files are provided for easy access, containing the atlas (v2) and the structural MRI (T2\*) and DTI (RGB-color FA map) template v1.01. The files are compatible with ITK-SNAP (version 3.0, not 3.2) and MBAT.

[\[back to top\]](#)

---

## References

Papp EA, Leergaard TB, Calabrese E, Johnson GA, Bjaalie, JG (2014) Waxholm Space atlas of the Sprague Dawley rat brain. *NeuroImage* 97, 374-386

Kjonigsen LJ, Lillehaug S, Bjaalie JG, Witter MP, Leergaard TB (2015) Waxholm Space atlas of the rat brain hippocampal region: Three-dimensional delineations based on magnetic resonance and diffusion tensor imaging. *NeuroImage*, in press